

## **Development and characterization of smart edible films**

**Eya Loukil**

Thesis report submitted to

**Escola Superior de Tecnologia e Gestão  
Instituto Politécnico de Bragança**

Master's Degree in  
**Chemical Engineering**

Within the scope of the double degree with the  
**Université Libre de Tunis**

Supervisors:

**Dr. Carla Pereira**

**Dr. Lillian Barros**

**Prof. Dr. Carolina Castilho Garcia**

**Prof. Dr. Dorsaf Cheikh**

Bragança

December 2023

## **ACKNOWLEDGEMENT**

My sincere thanks go to all those who have contributed to the completion of this thesis.

First and foremost, I would like to express my gratitude to Allah, the Most Merciful and the Most Compassionate, for His blessings and grace that have made this work possible. Throughout this journey, I have gained a deep understanding of myself, both academically and personally, and I am grateful for every opportunity, challenge, and ease that has been granted to me.

I would also like to acknowledge the importance of my esteemed supervisors, namely Carla Peireira, Lillian Barros, Carolina Castilho Garcia, Dorssaf Cheikh, and especially Maria Gabriela, for their valuable guidance, patience, and commitment throughout the research and writing process of this thesis. Their advice, laboratory assistance, constant encouragement, and contribution to the writing have been invaluable.

I warmly thank Maria Gabriela, a PhD student, for her practical advice, involvement in writing and statistical analysis, as well as for the quality of her work. Her patience and unwavering support have been of invaluable help.

I would like to express my gratitude to the members of CIMO for their kindness and assistance. Their collaboration has been precious.

My family has played an essential role in the pursuit of this work. Their advice and support have been invaluable, and I thank my parents, my brother Ghassen, and my sister Ghada for their love and valuable advice.

My friends also deserve special thanks for their constant support. I would like to express my gratitude to Ilyes and all others who have accompanied me throughout this journey.

Finally, I would like to thank all those who, directly or indirectly, have contributed to the success of this thesis. Your efforts and support have been greatly appreciated.

## ABSTRACT

Packaging is a very important tool to prevent food waste and ensure the product desired quality along shelf life. Beyond protecting foodstuff and helping to store it in hygienic conditions, packaging can also be helpful in indicating the overall condition of the contained food. These systems that monitor/communicate food quality and safety are known as smart/intelligent packaging and are increasingly used in food industry. However, a large amount of packaging is derived from synthetic polymers and represents a major obstacle to the sustainable development of a country, as it causes several negative impacts on nature for being nonbiodegradable. In this context, biodegradable packaging that could also permanently indicate the quality status of a product and share this information with the consumer is a challenger innovation path in food science with great potential to be absorbed in the industry. A possible way to detect food deterioration is through pH changes, which can be caused by various factors as microbial spoilage or oxidation mechanisms, among others. Through the addition of compounds that undergo easily detectable coloration changes with pH variation, as anthocyanins, biodegradable smart films can be developed, which was the main goal of this project.

To obtain the edible films, cassava starch was used together with glycerol, an important plasticizer, and anthocyanin-rich extract obtained from *P. spinosa* epicarp was also added to act as a pH indicator. The extract, obtained under previously optimized conditions, was tested for its chromatographic and bioactive profile. The most abundant anthocyanin compounds were cyanidin-3-*O*-rutinoside ( $[M+H]^+$  at  $m/z$  595) and peonidin-3-*O*-rutinoside ( $[M+H]^+$  at  $m/z$  609), presenting a total anthocyanin content of  $8.05 \pm 0.07$  mg/g of extract. The extract also showed great antimicrobial activity, mainly against *Salmonella enterica*, with a MIC of 2.5 mg/mL, and against *Escherichia coli*, *Staphylococcus aureus*, and *Aspergillus fumigatus* with a MIC of 5 mg/mL. In addition, it showed a strong antioxidant activity against lipid peroxidation (TBARS assay), with an  $EC_{50}$  value thirteen times lower than that presented by the positive control, Trolox ( $10.4 \pm 0.5$  and  $139 \pm 5$   $\mu$ g/mL, respectively). These results support to the potential use of the extract in smart films.

For the films formulation based on cassava starch and glycerol dissolved in water, five studies were selected from the literature. The formulations were reproduced to define the ideal conditions. Two good formulations were achieved: with 0.5 g or 0.8 g of glycerol, in 100 g of water, 3 g of cassava starch, and 1 g of anthocyanins. For control samples,

anthocyanin-rich extracts were not added. By testing different formulations, it was possible: to save energy, by choosing the lower temperature tested (70 °C) for gelation process; to save the degassing process by not forming bubbles at this temperature; and to verify the influence of each condition in the film formation process. The gelation temperature and relative humidity control during the drying process had the most important influence on the success of film manufacturing. Subsequently, the visual effects observed by varying the proportions of the ingredients were supported by FTIR and SEM evaluation. Overall, it was possible to conclude that the formulations presented good homogeneity and cohesion. The increase in glycerol from 16.6 to 26.6 g/100g of starch affected some bands in the FTIR spectra, also being observed by lower surface resistance by SEM. As for the addition of anthocyanins, this factor did not cause a major impact on the FTIR spectra and, despite resulting in rougher surfaces evaluated by SEM, the extract is applicable to films.

Furthermore, when tested in different pH solutions, the colour of the films was effectively changed, thus reinforcing the applicability of the anthocyanin extract in films based on cassava starch and glycerol, with potential application for monitoring pH changes in food products.

# INDEX

ACKNOWLEDGEMENT .....	ii
ABSTRACT .....	iii
INDEX.....	v
LIST OF TABLES.....	vii
LIST OF FIGURES .....	viii
1. INTRODUCTION.....	1
1.1. THE CONVENTIONAL PACKAGING PROBLEMATIC .....	1
1.1.1. THE LARGE USE OF PLASTIC .....	1
1.1.2. ENVIRONMENTAL AND HEALTH IMPACTS .....	2
1.2. NATURAL ALTERNATIVES OF PACKAGING MATERIALS.....	4
1.2.1. GENERAL ASPECTS.....	4
1.2.2. BIODEGRADABLE FILMS .....	7
1.3. DEVELOPMENT OF A FILM BASED ON CASSAVA STARCH AND ANTHOCYANINS.....	8
1.3.1. CASSAVA STARCH.....	9
1.3.2. ANTHOCYANIN-RICH EXTRACT FROM “PRUNUS SPINOSA” .....	10
1.3.3. INNOVATIONS AND CHALLENGES .....	12
2. OBJECTIVES.....	13
3. METHODOLOGY .....	14
3.1. PRUNUS SPINOSA L. FRUIT.....	14
3.2. PRUNUS SPINOSA L. EXTRACT .....	14
3.3. ANTHOCYANIN PROFILE .....	14
3.4. BIOACTIVE PROPERTIES OF THE EXTRACT.....	15
3.4.1. ANTIOXIDANT ACTIVITY .....	15
3.4.2. ANTIBACTERIAL ACTIVITY.....	16
3.4.3. ANTIFUNGAL ACTIVITY.....	17
3.5. FILM FORMULATIONS.....	18
3.5.1. PRELIMINARY STUDY .....	18
3.5.2. FINAL FILM FORMULATIONS.....	19
3.6. FILM CHARACTERIZATION.....	20
3.6.1. THICKNESS.....	20

3.6.2.	<i>MORPHOLOGY AND STRUCTURAL CHARACTERIZATION</i> .....	20
3.6.3.	<i>pH SENSITIVITY</i> .....	21
3.7.	STATISTICAL ANALYSIS.....	21
4.	RESULTS AND DISCUSSION.....	21
4.1.	EXTRACT CHARACTERIZATION.....	21
4.1.1.	<i>ANTHOCIANIN PROFILE</i> .....	21
4.1.2.	<i>BIOACTIVITIES</i> .....	23
4.2.	FILM FORMULATIONS.....	24
4.3.	FILM CHARACTERIZATION.....	27
4.3.1.	<i>THICKNESS</i> .....	27
4.3.2.	<i>FOURIER-TRANSFORM INFRARED SPECTROSCOPY (FTIR)</i> .....	27
4.3.3.	<i>SCANNING ELECTRON MICROSCOPE (SEM)</i> .....	34
4.3.4.	<i>pH SENSITIVITY</i> .....	36
5.	CONCLUSIONS .....	39
6.	REFERENCES .....	40

## LIST OF TABLES

<b>Table 1:</b> Active packaging described in literature and its applicability. ....	5
<b>Table 2:</b> Example of application of intelligent film based on anthocyanins colour change. Adapted from (Qin et al., 2019). ....	10
<b>Table 3.</b> Final film formulations. ....	19
<b>Table 4.</b> Anthocyanin tentative identification and quantification (in $\mu\text{g/mL}$ ). ....	22
<b>Table 5.</b> Antioxidant activity of the <i>Prunus spinosa</i> extract (in $\mu\text{g/mL}$ ). ....	23
<b>Table 6.</b> Antibacterial activity of the <i>Prunus spinosa</i> extract (in $\text{mg/mL}$ ). ....	24
<b>Table 7.</b> Antifungal activity of the <i>Prunus spinosa</i> extract (in $\text{mg/mL}$ ). ....	24
<b>Table 8.</b> Films based on cassava starch and glycerol for preliminary study. ....	19
<b>Table 9.</b> Thickness of the film formulations. ....	27
<b>Table 10.</b> Effects in the colour of the film immersed in different buffer solutions. ....	37

## LIST OF FIGURES

<b>Figure 1.</b> Cassava starch and its polymer structures. ....	9
<b>Figure 2.</b> <i>Prunus spinosa</i> L. shrub and fruits. ....	11
<b>Figure 3.</b> Anthocyanin chromatographic profile of the epicarp extract of <i>P. spinosa</i> fruits, obtained by HPLC-DAD at 520 nm. ....	22
<b>Figure 4.</b> FTIR spectrum of cassava starch. ....	28
<b>Figure 5.</b> FTIR spectrum of glycerol. ....	28
<b>Figure 6.</b> FTIR spectrum of the anthocyanin extract obtained from <i>P. spinosa</i> fruit epicarp. ....	29
<b>Figure 7.</b> Comparison of FTIR spectra of the film “0.5g-Control”, the glycerol and the cassava starch. ....	30
<b>Figure 8.</b> Comparison of FTIR spectra of the film “0.8g-Control”, the glycerol and the cassava starch. ....	31
<b>Figure 9.</b> Comparison of FTIR spectra of the film “0.5g-Anthoc”, the glycerol, the cassava starch, and the anthocyanin extract obtained from <i>P. spinosa</i> epicarp. ....	32
<b>Figure 10.</b> Comparison of FTIR spectra of the films “0.5g-Anthoc” and “0.5g-Control”. ....	32
<b>Figure 11.</b> Comparison of FTIR spectra of the film “0.8g-Anthoc”, the glycerol, the cassava starch, and the anthocyanin extract obtained from <i>P. spinosa</i> epicarp. ....	33
<b>Figure 12.</b> Comparison of FTIR spectra of the films “0.8g-Anthoc” and “0.8g-Control”. ....	34
<b>Figure 13.</b> SEM of the surface of starch-based films incorporated with anthocyanin extract. ....	35
<b>Figure 14.</b> SEM of the cross-section morphology of starch-based films incorporated with anthocyanin extract. ....	36
<b>Figure 15.</b> Effects in the colour of the film immersed in different buffer solutions. ....	37

# 1. INTRODUCTION

## 1.1. THE CONVENTIONAL PACKAGING PROBLEMATIC

### 1.1.1. *THE LARGE USE OF PLASTIC*

Packaging is a very important tool in the food supply chain, being part of production, distribution, and logistics, playing roles in preservation, storage, handling, and transportation. As it is the consumers' first contact, it is also essential in the merchandising, selling, and using goods, being described by Saha et al. (2022) as “the last output of production and the first input of marketing”.

The use of packaging has been reported since the dawn of humanity, with materials from clay, wood, bamboo, and leaves, followed by the production of pottery, paper, and glass. Then, the fragility of glass bottles gave way to the use of metal cans, until plastic began to be also widely used after the World War II (Risch, 2009).

Currently, it is clear that the food supply chain is dependent on plastic use. In every point of purchase, it is easy to find a large number of plastics, either as primary packaging, for the protection and supply of the final product, or as secondary or tertiary packaging, for grouping, transport, or containing the product. Considering different purposes of this material, Geyer et al. (2017) pointed packaging as the largest market of plastic, motivated from the reusable to single-use containers, where approximately 42% of all non-fiber plastics ever made have been used for packaging. This predominance was also recorded in plastic production of 2021, when 390.7 million metric tons (Mt) of plastic were produced globally, of which 44% were destined for packaging, followed by 18% for building & construction applications (PlasticEurope, 2022). Regarding the European production in the same year, 39.1% of the 50.3 Mt total plastic produced in the continent was to meet the packaging demand (PlasticEurope, 2022).

As published by Manalil et al. (2011), the food sector demanded 50% of the global packaging consumption, and about the total packaging, just rigid plastic represented 27% of this market. This is due to the advantages presented by this material in its different compositions, such as cost, malleability, resistance, transparency, and barrier properties to oxygen and humidity.

Among the types of plastic materials most commonly used for packaging beverages and food, thermoplastics, more specifically high-density (HDPE) and low-density (LDPE) polyethylene, polypropylene (PP), polystyrene (PS), polyvinylchloride (PVC), and poly-

ethylene terephthalate (PET) can be found. These have the characteristics of flexibility, softness, and are malleable when hot, in addition to being easily recyclable. However, thermoset and elastomer plastics are not recyclable, with the first one being the rigids, which can only be molded once when exposed to heat, and the second being elastic, with great stretching capacity, returning to its original shape after being stretched (Arcos Coba & Marín Cucalón, 2021).

All the versatility of using plastic for the various intended forms of packaging, in format, colours and functionality, associated with its low cost compared to other materials, made it a high cost-effective resource widely exploited and difficult to replace (Rossi & Bianchini, 2022). However, along with qualities, several damages are associated with the exacerbated use of plastic, among them, strong environmental impacts and harm to human health, which are discussed below (see 1.2.). Given these negative effects, seeking natural alternative sources for obtaining packaging materials that meet current needs and reduce the plastic dependence became a huge challenge.

### *1.1.2. ENVIRONMENTAL AND HEALTH IMPACTS*

The convenience in using plastic makes this material wildly used all over the world. The various problems involved in the use of this material begin with its composition, since they are produced from petroleum derivatives, a non-sustainable fossil resource. Moreover, the long molecular chains that constitutes plastic, called polymers, do not degrade naturally or take long periods to degrade, reaching up to 500 years. This condition generates a large accumulation in nature, with a negative impact on the environment and human health.

Through a global analysis of all mass-produced plastics ever manufactured (Geyer et al., 2017), until 2015, almost 5000 Mt of plastic waste were estimated to be accumulated in landfills or the natural environment. The short lifespan of plastic packaging promotes this huge volume of discard, since most of them are for single use.

When in landfills, plastic waste face improper management, with poor sorting of a portion that could be recycled, as well as materials that have toxic additives and that should be handled with caution (Hahladakis et al., 2018). Moreover, a considerable portion of the plastic waste that goes to landfills is lost in the environment (by processes such as wind, flooding, precipitation, or removed by animals) and burden the marine and terrestrial ecosystems (Yadav et al., 2020). Lebreton et al. (2018) predicted that an amount of at least 79 (45–129) thousand tonnes of plastic is floating in an ocean area of 1.6 million km<sup>2</sup>.

Incineration and recycling are other routes for the disposal of plastic waste. However, when plastic is openly burned, it emits polluting gases, as carbon monoxide (CO) and carbon dioxide (CO<sub>2</sub>) (Hahladakis et al., 2018). Although recycling is an important strategy to reduce the production of virgin plastic and the amount of plastic waste, only about 9% of all plastic generated goes to recycling, and of these only 10% have been recycled more than once (Geyer et al., 2017). In addition, recycling plastic materials faces some challenges to obtain a high purity mono polymer (at least 99.98% purity required), such as removing all external contamination (e.g., glue and dirt) and desorbing any remaining substances (Harrison & Hester, 2018), conditions that limit the technical and economic value of the recycled material. Actually, considering the European strategy for plastics in a circular economy, that aims to increase the capacity of recycling of plastics in the Union and consequent reduction of the adverse impacts of plastic pollution, the Commission Regulation (EU) 2022/1616 entered in force on 10 October 2022, directing the use of recycled plastic materials and articles intended to be in contact with food (Commission Regulation (EU) 2022/1616, 2022).

In Europe, the Regulation (EC) N° 1935/2004 determines the safety and inertness for all Food Contact Materials (FCMs). But not all plastic materials intended for food packaging meet the requirements, and there are concerns about the migration of plastic additives and non-intentionally added substances (NIAS), and their potential health risk (Kim et al., 2023; Pack et al., 2021). Factors such as heating, especially in microwaves, favour the migration of compounds from packaging to food (Pack et al., 2021). A relevant problem example is bisphenol A (BPA), a compound widely used in plastic packaging, but which migrates to food and is absorbed by consumers, being associated with kidney, endocrine, and reproductive problems (Deba & Núñez, 2017; Lora et al., 2010; Mas et al., 2017).

Another plastic problem is related to microplastics, which are all those with less than 5 mm in length, as defined by the National Oceanic and Atmospheric Administration (NOAA, 2023). Those microplastics result from primary production, usually from industrial, cosmetic products and maritime transport waste, or else of secondary origin, being debris formed in the degradation processes of larger pieces of plastic into smaller ones.

In addition to the different destinations given to plastic waste, the various plastic forms circulate in the environment. Microplastics are transported from landfills to soils and rivers through leaching, flooding, and wind, or are dumped in untreated sewage, or when treated, do not have sufficient capacity to remove plastics smaller than 100 µm. A

representative part of the microplastics present in sewage system is from textile, by washing fabrics, and also from cosmetic products, such as facial cleansers and toothpastes, among other factors such as degradation of packaging, automotive tires, discards on vessels, oil platforms, aquaculture, shopping bags, paints, etc. (Mamun et al., 2023). Consequently, the presence of this material in nature affects terrestrial and aquatic life. For example, deaths from starvation have been reported (Sarria-Villa & Gallo-Corredor, 2016), which happens when animals ingest microplastics and this causes an obstruction of the digestive system, as well as the inhibition of the photosynthesis process in algae due to the interference of nanoplastics. Microplastics and nanoplastics present in water, absorbed by plants, and ingested by animals such as fish and bees, also affect the human food chain. When inhaled and ingested, these materials can be absorbed through the intestinal tract and present toxicity, affecting the central nervous system and the reproductive system (Sarria-Villa & Gallo-Corredor, 2016; Waring et al., 2018).

## 1.2.NATURAL ALTERNATIVES OF PACKAGING MATERIALS

Faced with the problem of finding alternatives that meet the needs of food packaging allied to the concern about the impacts on the environment and consumers' health, the scientific community has been studying different natural matrices and innovative applications, to replace the plastic materials, avoiding their negative aspects previously discussed.

### 1.2.1. GENERAL ASPECTS

In a brief search through the literature, several innovative strategies for the use of packaging to protect and increase the shelf life of food can be found, although many of them still depend on plastic materials, as shown in **Table 1**. With the improvement of packaging over the years, mixtures of materials have been made, as well as the use of additives, multilayers and coatings, reaching an increased efficiency of the functionality of the packaging. Likewise, the active packaging, which are those that intentionally interact with the product, started to gain interest. An old example is the microwave popcorn bag that, in mid-1980s, received a metalized PET film (susceptor) laminated between the layers of paper, that interacts with the microwave energy, ensuring the necessary heating for the popping of the grains (Risch, 2009).

**Table 1.** Active packaging described in literature and its applicability.

Packaging	Natural bases	Unnatural Bases	Active advantages	Tested applicability	References
Multilayer film	- Chitosan coating solution in acetic acid solution or Alginate coating solution in distilled water - Black cumin oil	Corona discharge treated polyethylene (PET) films (PEF)	Antimicrobial activity	The film provided lower microbial growth, less variation in pH, and lower colour changes in the tested chicken breast meats during 5 days of storage at 4 °C.	(Konuk Takma & Korel, 2019)
Film	Citral and trans-cinnamaldehyde encapsulated in $\beta$ -Cyclodextrin	Ethylene vinyl alcohol copolymer (EVOH)	Antimicrobial activity	Formulated films showed better stability and controlled release of bioactive agents. The EVOH film with $\beta$ -Cyclodextrin-Citral complex extended the shelf life of beef shank about 4 days when stored at $4 \pm 1$ °C.	(Chen et al., 2019)
Film	Solution of commercial food grade lipid soluble rosemary extract containing 4.5% of carnosic acid in ethanol	Low density polyethylene (LDPE)	Antioxidant activity	Limited the lipid oxidation induced by high pressure processing in pork patties stored at 5 °C for 60 days.	(Bolumar et al., 2016)
Film	Essential oils (carvacrol and thymol mixtures) entrapped within halloysite nanotubes	Low density polyethylene (LDPE)	Antimicrobial activity	The films have completely eradicated <i>E. coli</i> in the tested hummus.	(Krepker et al., 2017)
Edible biofilm	- Grapefruit essential oil - Plum seed protein isolates - Gum acacia - Glycerol	—	Preservative activity	All the films containing the grapefruit essential oil demonstrated antimicrobial effect against <i>E. coli</i> , while the radical scavenging activity was related to the essential oil concentration released from the film.	(Li et al., 2020)
Edible biofilm and coating	- Opuntia cladodes mucilage - Locust bean gum - Polyphenols from Opuntia cladodes - Glycerol (for the film)	—	Antioxidant capacity	The obtained biofilm showed antioxidant power as well antiradical action in aqueous food simulat. The application of the film as coating (without glycerol) on refrigerated apples for 9 days preserved their organoleptic properties, mitigating weight loss and pH regression, without losing a good soluble solids rate.	(Sarra & Ilham, 2022)
Edible coating	- Commercial bovine gelatine - Chitosan in acetic acid 0.4% - Glycerol	—	Colour preservation	The coating effectively decreased the weight loss, lipid oxidation, and discolouration of coated steaks during 5 days of retail display.	(Cardoso et al., 2016)
Coating	Suspension of bentonite	Potassium sorbate	Preservative activity	Mangos treated with the coatings exhibited reduced decay, delayed postharvest ripening, decreased water loss, maintained high vitamin C levels, preserved titratable acidity, and no changes in flavour.	(K. Liu et al., 2014)

Currently, with the improved technology and the different techniques available for forming films, coatings and multilayers, the development of active packaging has been increasingly explored, even prioritizing the use of natural compounds and a lower environmental impact. In this sense, **Table 1** presents some advances in obtaining active packaging and their tested advantages in food protection. Obtaining all-natural packaging is specifically discussed below (see 2.2.).

The use of techniques that incorporate natural ingredients into widely used plastic materials has been verified with a consequent increase of the product shelf life. Konuk Takma & Korel (2019) and Chen et al. (2019) achieved antimicrobial activity in plastic films through different methodologies. In the first study, the authors immersed polyethylene successively in alternating solutions of alginate and chitosan added with black cumin oil. On the other hand, Chen et al. (2019) mixed EVOH resin, antimicrobials, and  $\beta$ -cyclodextrin using a single-screw extruder. Both films prolonged shelf life of meat. Also, antioxidant properties have been attributed to low density polyethylene (LDPE), by spreading a rosemary extract (Bolumar et al., 2016), and antimicrobial activity by shear mixing of a synergistic mixture of essential oils with halloysite nanotubes followed by ultrasonication (Krepker et al., 2017).

Another relevant strand is the intelligent packaging that communicates the condition of the product, for example the pathogen indicators, by reaction with toxins, and freshness indicators, by reaction with pH change or with (non-) volatile metabolites (Fang et al., 2017). Recently, Weston et al. (2020) developed a colorimetric sensor, using a polydiacetylene/zinc oxide system, that indicates the milk freshness without the need to open the package. The system monitors the milk pH based on lactic acid concentration, an indicator of bacterial spoilage. In this sense, Heising et al. (2012) developed a non-destructive method for monitoring changes in the headspace ammonium of packed fish. The freshness status is indicated by electrodes that in an aqueous phase in the package monitor changes in the concentration of ammonia produced. Meanwhile, glucose was purposed for the identification of beef meat freshness, using a glassy carbon electrode modified with multi-walled carbon nanotubes and chitosan (Uwimbabazi et al., 2017).

All these technologies aim to promote better food preservation, increasing their shelf life, reducing waste, and preventing consumers' health issues. However, a higher challenge is proposed with the use of natural matrices with lower environmental impacts.

### 1.2.2. BIODEGRADABLE FILMS

Different polymers can be obtained from natural sources, such as (Mangaraj et al., 2018): i) extraction of polysaccharides from potato, corn, rice, cotton, wood, guar, algae, locust bean, and others; ii) extraction of proteins from animals, plants, whey, soy, and other; iii) extraction of lipids from waxes, fat, and oils; iv) production by microorganisms, as cellulose and xanthan.

These biopolymers are being widely investigated as a solution for the problems presented by plastics, as they easily degrade and are obtained from renewable sources, causing less damage to the environment, but still presenting the properties of conventional polymers (Mangaraj et al., 2018; Siracusa et al., 2008).

The characteristics expected from the polymers change regarding their application. For example, a low water vapour transmission rate is important for preserving bakery products, but favour the dehydration in fresh fruits. The different barrier properties as gases, water vapour, organic vapours and liquid, as well the mechanical and chemical resistance properties need to be established and evaluated (Siracusa et al., 2008).

Li et al. (2020) developed a natural and edible film based on plum seed protein isolate, gum acacia conjugates, and glycerol. They also added grapefruit essential oil in order to promote an active effect in the film. In addition to antioxidant and antimicrobial activity achieved with this ingredient, 1 to 4% of essential oil content also improved the water vapor barrier property, surface hydrophobicity, mechanical properties, and thermal stability of the film. In another study, the authors formulated a film based in potato starch, clay and glycerol, in which the sorbate potassium addition increased water permeability and elongation at break of the films and decreased tensile strength, also promoting antimicrobial activity, when in higher contents.

Promising results in replacing the traditional use of polyethylene plastic films (PE) were obtained from Liu et al. (2023), when comparing the use of chitosan/bacterial cellulose composite films added with curcumin in the food preservation. In that study, the developed biodegradable film showed higher preservation of strawberries and significantly slowed the oxidation of edible oils.

Also, the biodegradability of natural-based films was easily verified: different formulations of mosambi peel and sago-based films were buried for 15 days in soil, with a reduction of weight ranging from  $46.45 \pm 0.39$  to  $64.42 \pm 0.22\%$  after this short time (Ahmad et al., 2022).

### 1.3.DEVELOPMENT OF A FILM BASED ON CASSAVA STARCH AND ANTHOCYANINS

Considering all the scenario previously described, the present work aims to develop a smart and biodegradable film based on cassava starch and anthocyanins, motivated by promising results of this interaction found in literature, despite its little exploitation.

Qin et al. (2019) used a solution of cassava starch and glycerol with the addition of *Lycium ruthenicum* anthocyanins to prepare films by the casting technique. According to the authors, the interaction of the starch and anthocyanins formed hydrogen bonds, which greatly improved the moisture content, water vapor permeability and mechanical strength of the films. In addition, the anthocyanin content provided active and intelligent properties to the film, retarding the oxidation process and monitoring the freshness of pork, also enhancing the light barrier.

On the other hand, Vedove et al. (2021) made thermoplastic starch packaging by extrusion. For that purpose, the solution of cassava starch and glycerol, acidified with stearic acid, was extruded using a co-rotating twin-screw extruder, producing pellets with 2 mm in length. Then, these pellets were extruded with the incorporation of an anthocyanin-rich solution, from grape skin, to obtain the films. In this study, the anthocyanins addition did not favour the mechanical properties of the film, suggesting the need for improvements in the packaging formulation. However, it was evidenced that, in the highest concentration of anthocyanins tested, the film presented intelligent properties, with potential as an indicator of freshness in the storage of beef and fish at 6 °C.

The powdered blueberry bagasse, an anthocyanin-rich matrix, was tested in the development of cassava starch-based films, through two different methods. In the first study (Luchese et al., 2018), the authors fabricated film by casting, using glycerol as a plasticizer. In the second one (Andretta et al., 2019), the film was made by thermocompression, with sorbitol plasticizer. In both studies, the results showed the potential use of starch-bioresidue films as food packaging with a pH indicator. Packaging films formulated with red cabbage extracts and dual-modified cassava starches also presented intelligent properties, in addition to high water-resistance and great tensile strength (Cheng et al., 2022).

### 1.3.1. CASSAVA STARCH

Cassava (*Manihot esculenta* Crantz) is a domesticated specie of starchy root vegetable or tuber, widely cultivated and consumed around the world. The starch is composed of two polymers, amylopectin and amylose (**Figure 1**), that gummify with more than 70 °C and excess of water, then forming films when cold, due to its retrogradation properties (Matheus et al., 2023; Vicentino et al., 2011). The cassava starch has been studied in the production of bioplastics due to its advantageous properties, including its biodegradability and renewable source, as well as for resulting in films with good oxygen barrier ability, stretchability, and suitable transparency (Matheus et al., 2023).

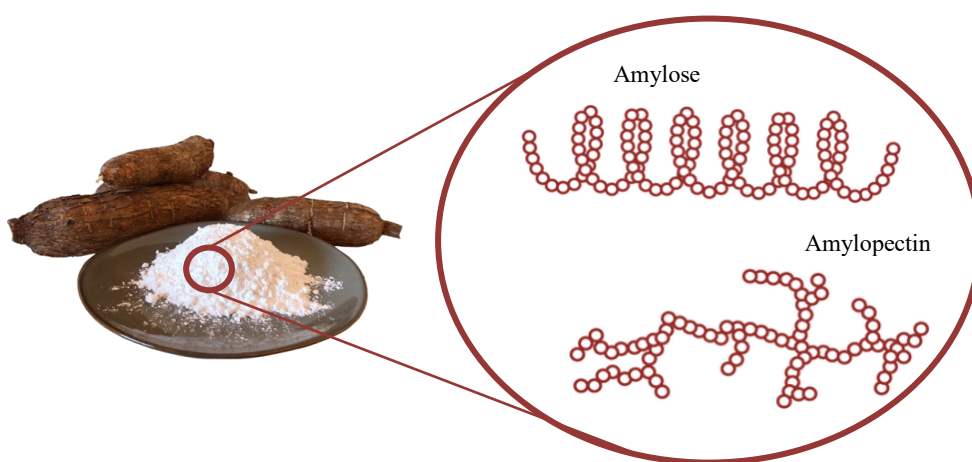


**Figure 1.** Cassava starch and its polymer structures.

The amylose content, which is more linear with few branches, contributes to the starch-film strength, while the amylopectin interferes in the mechanical properties of the film, due to its highly branched structure (Ezeoha & Ezenwanne, 2013). Although currently commercially available, starch-based films present some challenges. This is because this biopolymer is very hydrophilic, which makes it technologically unfavourable for application in food packaging that requires water resistance. However, these conditions can be improved by blend with other biopolymers, adding plasticizers such as sorbitol and glycerol, and/or additives.






















In the formulation of cassava starch films with the addition of sorbitol and glycerol in different proportions, it was observed that, due to the ability of glycerol to retain water through the formation of hydrogen bonds, thicker films were obtained when plasticized with high glycerol content. Also, the greater ability of glycerol to interact with water molecules in starch, comparing with sorbitol, resulted in low tensile strength in the film with the higher

content of glycerol (Lim et al., 2020). Moreover, the intermolecular interactions by hydrogen bonds between anthocyanins and cassava starch significantly enhanced the water vapor, ultraviolet-visible light barrier ability, and tensile strength (Qin et al., 2019).

### 1.3.2. ANTHOCYANIN-RICH EXTRACT FROM “PRUNUS SPINOSA”

Anthocyanins are water-soluble colouring compounds widely found in nature in fruits and vegetables. The colour of these molecules is pH dependent, being an important parameter since the colours of anthocyanins reversibly change with pH variations. Anthocyanins are more stable at acidic pH and, as this increases, the ionic nature of anthocyanins promotes changes in their molecular structure, resulting in different colours. This colour variation in anthocyanins makes them a promising additive to be used in packaging films, as an indicator of food freshness. The idea is that, as the pH of the food changes due to the deterioration/contamination process, the colour of the anthocyanin-based film also changes and makes it possible to identify the spoiled state of the food product without opening the packaging (Zhao et al., 2022). As an example, **Table 2** shows the remarkable colour changes according to pH variation of starch-film with different contents of *L. ruthenicum* anthocyanins used to monitor the freshness of pork.

**Table 2.** Example of application of intelligent film based on anthocyanins colour change. Adapted from (Qin et al., 2019).

Time (h)	pH value of pork meat	Starch-films with different contents of <i>L. ruthenicum</i> anthocyanins		
		1%	2%	4%
0	5.96 ± 0.01			
8	6.10 ± 0.02			
16	6.15 ± 0.02			
24	6.49 ± 0.01			
32	6.65 ± 0.01			
40	6.96 ± 0.05			
48	7.45 ± 0.01			

In addition to the property of changing colour with pH variations, these molecules also present valuable bioactive properties that can be exploited in obtaining intelligent and active films. Indeed, anthocyanins have well-known antioxidant and antimicrobial capacity, so, when migrating from the packaging to the food, these compounds can even act as preservative agents (Wang et al., 2023).

*Prunus spinosa* L. (blackthorn; **Figure 2**) is a wild shrub which fruits are rich in anthocyanins, more specifically cyanidin 3-rutinoside and peonidin 3-rutinoside.



**Figure 2.** *Prunus spinosa* L. shrub and fruits.

A previous optimization study of the extraction process of blackthorn fruit epicarp (Leichtweis et al., 2019) suggested the ultrasound-assisted extraction as the most effective method to obtain anthocyanins, when compared to the heat-assisted extraction, in the conditions of  $5.00 \pm 0.15$  min,  $400.00 \pm 32.00$  W, and  $47.98\% \pm 2.88\%$  of ethanol, allowing an extraction yield of 18.17 mg of anthocyanins per g of extract. The colouring capacity of the optimal extracts was confirmed in a typical Brazilian bakery product, “beijinhos”, and the bioactive potential was also verified, with the extracts presenting great antioxidant and antimicrobial activity before and after their incorporation into the food matrix (Backes et al., 2020).

Considering these results, *P. spinosa* fruit epicarp extract can be perceived as a promising source of anthocyanins to be applied in cassava starch-films to confer them active and intelligent properties.

### *1.3.3. INNOVATIONS AND CHALLENGES*

Despite the growing interest in using cassava starch in food packaging, the development of an effective biodegradable film to be applied in food preservation and monitoring is still scarce. In addition, it was found that, by 2022, only 37.65% of studies of cassava starch films assessed the performance of those films as food packaging (Matheus et al., 2022).

Considering the review carried out in the present state of the art, the proposed challenge is to find a formulation containing cassava starch and anthocyanin extracts that can form a film suitable for food packaging with active and intelligent properties, thus contributing with an innovative solution for a more sustainable food supply chain.

## 2. OBJECTIVES

The present study aimed to develop a biodegradable food packaging based on cassava starch and anthocyanin extracts.

The specific objectives were:

- To develop films using cassava starch, glycerol, and anthocyanin extracts obtained from *P. spinosa* fruit epicarp, through the casting method;
- To assess the physical properties of the developed films, aiming its application as food packaging;
- To evaluate the applicability of the films as indicators of pH variation by changing their colour.

### 3. METHODOLOGY

#### 3.1. *PRUNUS SPINOSA* L. FRUIT

*Prunus spinosa* L. fruits were harvested in Bragança, Portugal, in October 2022. After harvest, the fruits were carefully peeled, and the epicarps were freeze-dried using a lyophilizer (Free Zone 4.5, Labconco). Once freeze-dried, these peels were ground into a powder with a particle size of 20 mesh and stored in a freezer at a temperature of -20 °C for further analysis.

#### 3.2. *PRUNUS SPINOSA* L. EXTRACT

The freeze-dried extracts were prepared following the best conditions established in previous studies (Backes et al., 2018; Leichtweis et al., 2019). The extraction was carried out using an ultrasonic device from QSonica (model CL-334, Newtown, Connecticut, United States). During the extraction process, the peels of *Prunus spinosa* were treated with a specific solvent. This solvent was a mixture composed of 50% ethanol and 50% water, with a concentration of 75 g/L and a pH adjusted to 3 using citric acid. The treatment was performed for a duration of 5 minutes, with an ultrasonic power of 400 W.

Once the extraction was completed, the samples were subjected to a centrifugation step at 6000 revolutions per minute for 20 minutes at a temperature of 10 °C. This step aimed to separate the suspended solids from the liquids. Then, the obtained liquids, called supernatants, were filtered through Whatman filter paper no. 4 to remove any remaining solid particles.

The supernatants, free from suspended particles, were freeze-dried to remove the moisture. The freeze-dried samples were stored at a temperature of -20 °C in a refrigerator for future analysis.

#### 3.3. ANTHOCYANIN PROFILE

The extract was re-suspended in ethanol:water (80:20 v/v), at a final concentration of 5 mg/mL, and filtered (0.2 µm). The anthocyanic profile was determined by liquid chromatography and mass spectrometry (HPLC-DAD/ESI-MS, Dionex Ultimate 3000 UPLC, Thermo Scientific, San Jose, CA, USA). The compounds identification was achieved following the protocol previously described by Bastos et al. (2015). Accordingly, the

separation was achieved on a reverse-phase C18 column from AQUA® (Phenomenex) (5 µm, 150 mm × 4.6 mm i.d) thermostated at 35 °C. The solvents used were: (A) 0.1% TFA in water and (B) 100% acetonitrile. The gradient used was: isocratic 10% B for 3 minutes, 10 to 15% B for 12 minutes, isocratic 15% B for 5 minutes, 15 to 18% B for 5 minutes, 18 to 30% B for 20 minutes, and 30 to 35% B for 5 minutes, at a flow rate of 0.5 mL/min. Detection was performed using DAD, with a preferred wavelength of 520 nm, and the MS equipment described previously. Zero-grade air was used as the nebulizer gas (40 psi), and turbo gas (600 °C) was used for solvent drying (50 psi). Nitrogen served as the curtain gas (100 psi) and collision gas (high). The ion spray energy was set at 5000V in positive mode. EMS and ESI methods were used for high-resolution spectra acquisition and precursor ion fragmentation patterns, respectively. The parameters defined for the EMS mode were: DP 41V, EP 7.5V, CE 10V, and the parameters for the EPI mode were: DP 41V, EP 7.5V, CE 10V, and collision energy spread (CES) 0V. The anthocyanins were characterized based on their UV and mass spectra and retention time, compared to the available standard. For quantitative analysis, 7-level calibration curves were obtained by injecting standard solutions with known concentrations (0.25-50 µg/mL): cyanidin-3-*O*-glucoside ( $y = 243287x - 1000000$ ,  $R^2=0.999$ ) and peonidin-3-*O*-glucoside ( $y = 447974x - 122417$ ,  $R^2=0.9999$ ). The results were expressed in mg of compound per g of extract.

### 3.4. BIOACTIVE PROPERTIES OF THE EXTRACT

#### 3.4.1. ANTIOXIDANT ACTIVITY

To evaluate the antioxidant activity of the extracts, the DPPH and TBARS methods were used, as described below.

For the TBARS method, the protocol described by Sarmiento et al. (2015) was used. The lyophilized hydroethanolic extracts were re-dissolved in ethanol:water (80:20, v/v) to obtain a 0.5 mg/mL stock solution, diluting successively to obtain six concentrations below it. A porcine brain suspension (*Sus scrofa*) was prepared, in which a portion of the brain was mixed with Tris-HCl buffer (20 mM, pH 7.4) in a ratio of 1:2 (m/v), centrifuging the mixture at 3500 rpm for 10 min at a temperature of 10 °C to prevent rancidification of the mixture. In eppendorf tubes, 200 µL of each of the solutions of extract were placed, adding 100 µL of ascorbic acid (0.1 mM), 100 µL of iron sulfate (FeSO<sub>4</sub> - 10 mM), and 100 µL of the supernatant homogenized from pig brain, incubating at 37.5 °C for 1 hour. After incubation, the reaction was stopped by adding 500 µL of trichloroacetic acid (28% m/v) and 380 µL of

thiobarbituric acid (2% w/v, TBA) was also added. The tubes were placed in a water bath at 80 °C for 20 minutes, in order to promote the reaction between TBA and malondialdehyde (MDA - reactive oxygen species resulting from lipid peroxidation that occurs in pig brain tissue). To separate the residues from the supernatant, the mixture was centrifuged for 5 min at 3500 rpm. The colour intensity of the MDA - TBA complex was measured at 532 nm. The percentage of inhibition of lipid peroxidation was calculated using the following equation:

% inhibition of lipid peroxidation =  $(A - B) / A \times 100$ , where A and B refer to the absorbance of the control (water) and the extract solution, respectively. The extract concentration corresponding to 50% inhibition of lipid peroxidation (IC<sub>50</sub>) was calculated from the graph of the percentage of inhibition of TBARS formation as a function of the extract concentration. As a positive control, Trolox was used and the results were expressed in µg/ml.

Regarding DPPH method, the radical-scavenging activity was assessed using a microplate Reader (Bio-Tek Instruments, Inc.; Winooski, USA). The reaction mixture in each of the 96 wells consisted of the extracts at different concentrations (30 µL) and methanolic solution (270 µL) containing DPPH radicals ( $6 \times 10^{-5}$  mol/L). The mixture was left to stand for 60 min in the dark and at room temperature. The absorbance was measured at 515 nm to assess the reduction of DPPH radicals, which was calculated as a percentage of DPPH discolouration using the formula:

$[(A_{\text{DPPH}} - A_{\text{S}})/A_{\text{DPPH}}] \times 100$ , where A<sub>S</sub> is the absorbance of the solution containing the sample, and A<sub>DPPH</sub> is the absorbance of the DPPH solution (Rita et al., 2016).

#### 3.4.2. ANTIBACTERIAL ACTIVITY

Regarding antibacterial activity, the extracts were tested against five Gram-negative bacteria, namely *Enterobacter cloacae* (ATCC 49741), *Escherichia coli* (ATCC 25922), *Pseudomonas aeruginosa* (ATCC 9027), *Salmonella enterica* subsp (ATCC 13076), and *Yersinia enterocolitica* (ATCC 8610) and three Gram-positive bacteria, namely *Bacillus cereus* (ATCC 11778), *Listeria monocytogenes* (ATCC 19111), and *Staphylococcus aureus* (ATCC 25923). All these microorganisms were purchase at Frilabo, Porto, Portugal. The bacteria were incubated at 37 °C in an appropriate fresh medium, for 24 h before analysis to maintain the exponential growth phase.

The MIC determination in all bacteria were conducted using a colorimetric assay, according to the described by Pires et al. (2018). The samples were, first of all, dissolved in 5% (v/v) dimethyl sulfoxide (DMSO) and 95% of autoclaved distilled water to give a final concentration of 20 mg/ mL for the stock solution. 90  $\mu$ L of this concentration was added in the first well (96-well microplate) in duplicate with 100  $\mu$ L of Tryptic Soy Broth (TSB). In the remaining wells, 90  $\mu$ L of TSB medium was added. Then, the samples were serially diluted to obtain the concentration ranges from 10 to 0.03125 mg/mL. To finish, 10  $\mu$ L of inoculum (standardized at  $1.5 \times 10^6$  Colony Forming Unit (CFU) /mL) was added to all the wells assuring the presence of  $1.5 \times 10^5$  CFU. Two negative controls were prepared, one with TSB and another one with the extract. Two positive controls were prepared: with TSB and each inoculum and another with medium, antibiotics, and bacteria. Ampicillin and Streptomycin were used for all bacteria tested and Meticilin was also used for *Staphylococcus aureus*. The microplates were incubated at 37°C for 24 h. The MIC of samples was detected following the addition (40  $\mu$ L) of 0.2 mg/mL *p*-iodonitrotetrazolium chloride (INT) and incubation at 37°C for 30 min. MIC was defined as the lowest concentration that inhibits the visible bacterial growth, determined by the change of the coloration from yellow to pink if the microorganisms are viable. For the determination of MBC, 10  $\mu$ L of liquid from each well that showed no change in colour was plated on solid medium, Blood agar (7% sheep blood) and incubated at 37°C for 24 h. The lowest concentration that yielded no growth, determine the MBC. MBC was defined as the lowest concentration required to kill bacteria.

#### 3.4.3. ANTIFUNGAL ACTIVITY

The antifungal activity was performed according to the described by Heleno et al. (2013). *Aspergillus brasiliensis* (ATCC 16404) and *Aspergillus fumigatus* (ATCC 204305) were used. The organisms were obtained from Frilabo, Porto, Portugal. The micromycetes were maintained on malt agar and the cultures stored at 4 °C, being further placed in new medium and incubated at 25°C for 72h. In order to investigate the antifungal activity, the fungal spores were washed from the surface of agar plates with sterile 0.85% saline containing 0.1% Tween 80 (v/v). The spore suspension was adjusted with sterile saline to a concentration of approximately  $1.0 \times 10^5$  in a final volume of 100  $\mu$ L per well. The samples were first of all dissolved in 5% (v/v) dimethyl sulfoxide (DMSO) and 95% of autoclaved distilled water to give a final concentration of 20 mg/ mL for the stock solution. Afterwards,

90  $\mu\text{L}$  of this concentration was added in the first well (96-well microplate) in duplicate with 100  $\mu\text{L}$  of Malt Extract Broth (MEB).

In the remaining wells, 90  $\mu\text{L}$  of medium MEB were placed. Then, the samples were serially diluted to obtain the concentration range of 10 to 0.03125 mg/mL. Minimum inhibitory concentration (MIC) determinations were performed by a serial dilution technique using 96-well microplate. The lowest concentrations without visible growth (at the binocular microscope) were defined as MICs. The fungicidal concentration (MFC) was determined by serial subcultivation of a 2  $\mu\text{L}$  of tested compounds dissolved in medium and inoculated for 72 h, into microplates containing 100  $\mu\text{L}$  of MEB per well and further incubation 72 h at 26 °C. The lowest concentration with no visible growth was defined as MFC indicating 99.5% killing of the original inoculum. Commercial fungicide ketoconazole (Frilabo, Porto, Portugal), was used as positive control.

### 3.5. FILM FORMULATIONS

#### 3.5.1. PRELIMINARY STUDY

For the preliminary study, to define the ideal conditions of the film formulation, five studies were selected based on cassava starch and glycerol dissolved in water. Each of the studies used protocols with considerably different parameters, despite the similarity of the process used and the results obtained by the authors in terms of the characteristics of the films. The parameters of the different films are described in **Table 3**.

In general, the casting method was used to obtain the films, which consists of pouring the gelled starch solution onto plates for subsequent drying. Control films were prepared by combining cassava starch, glycerol, and 100 g of distilled water, manually mixed in this order. To the smart films, the extract rich in anthocyanins was dissolved at this stage in the mixture. Once the mixture was ready, it was placed in a heating bath with continuous stirring to achieve the temperature assumed by protocols. Afterwards, the mixture was removed from the heating bath. Then, the film-forming solution was applied to the Petri dish to dry with monitoring of temperature and relative humidity, for a determined time, as described in **Table 3**. The samples were stored in a desiccator containing silica, at room temperature, until further analysis (maximum 24 h).

**Table 3.** Films based on cassava starch and glycerol for preliminary study.

Parameters	Films				
	1	2	3	4	5
<i>Conditions to preparer the film-forming solution</i>					
Starch (g/100 g of water)	4	5.34	3	4	2
Glicerol (g/100 g of starch)	25	28	15 and 40	20	25
Temperature (°C)	90	96	95	95	70
Time of heating (min)	5	40	10	10	1
<i>Conditions to dry the films</i>					
Temperature (°C)	30	50	40	40	30
Time	48h	48h	Until constant weight	24 h	18-20h
RH (%)	50	Room RH	Not informed	Not informed	60 ± 5
Reference	Yun et al. (2019)	Medina-Jaramillo et al. (2017)	Shimazu et al. (2007)	Queiroz et al. (2021)	Vicentini (2003)

### 3.5.2. FINAL FILM FORMULATIONS

After a thorough evaluation of the different film formulations (see 4.2), it was possible to define two promising final formulations, described in **Table 4**. The formulations consisted of mixing 3 g of starch with 0.5 or 0.8 g of glycerol and dissolving in 100 g of distilled water. For the smart film, 1 g of anthocyanin extract was also added. The mixture was heated until 70 °C, remaining at that temperature for 1 min. Then, 20 g of film-forming solution was placed in Petri dishes to dry in the oven at 40 °C and 50 % of relative humidity, for 48 h. The samples were stored in a desiccator at room temperature until further analysis.

**Table 4.** Final film formulations.

Parameters	Films	
	1	2
<i>Conditions to preparer the film-forming solution</i>		
Starch (g/100 g of water)		3
Glycerol (g/100 g of starch)	16.6	26.6
Anthocyanins (g/100 g of starch)		33.3*
Temperature (°C)		70
Time of heating (min)		1
<i>Conditions to dry the films</i>		
Temperature (°C)		40
Time (h)		48
RH (%)		50

\* No anthocyanin extract was added to the control formulation.

For better understanding, the films were coded as follows:

- “0.5g-Control”: film that contains 0.5 g of glycerol (16.6 g/100 g of starch);
- “0.8g-Control”: film that contains 0.8 g of glycerol (26.6 g/100 g of starch);
- “0.5g-Anthoc”: film that contains 0.5 g of glycerol (16.6 g/100 g of starch) and 1 g of anthocyanin extract (33.3 g/100 g of starch);
- “0.8g-Anthoc”: film that contains 0.8 g of glycerol (26.6 g/100 g of starch) and 1 g of anthocyanin extract (33.3 g/100 g of starch);

## 3.6. FILM CHARACTERIZATION

### 3.6.1. THICKNESS

The determination of the film thickness is a fundamental step in the characterization of smart films because it directly influences many properties and performances of the films, such as their mechanical strength, barrier capacity, flexibility, and many others (Lin et al., 2022).

To measure the film thickness, we used a well-established metrology tool, a digital micrometre, which consists of two jaws, one fixed and the other movable, which can be moved relative to each other to accurately grasp and measure the film thickness by placing it between the jaws of the instrument and reading the displayed value on the graduated scale. To ensure accurate measurements, we ensured that the film was properly positioned, and that the micrometre was regularly calibrated. The thickness was measured at three different points of each sample.

### 3.6.2. MORPHOLOGY AND STRUCTURAL CHARACTERIZATION

The surface and cross-section of the films, both with and without anthocyanin extract, were analyzed using a scanning electron microscope (SEM; JEOL, model JSM 6700). Before measurement, a layer of gold was sputtered onto the samples.

Fourier transform infrared spectroscopy (FTIR) was conducted on the film samples, again with and without anthocyanin extract, using a Thermo Fisher Scientific Nicolet 6700 spectrometer (MA, USA). The spectra were captured within the range of 400 to 4000  $\text{cm}^{-1}$  at a resolution of 4  $\text{cm}^{-1}$ , and each spectrum was obtained through 34 scans.

### 3.6.3. pH SENSITIVITY

Film samples were immersed in different pH buffers (ranging from 1 to 12) at room temperature, and natural reaction was allowed to occur (about 30 min). After this, colour was measured at three different points of each sample using a colorimeter (model CR-400, Konica Minolta Sensing Inc.). Illuminant C and a diaphragm aperture of 8 mm were used, where CIE colour space values L\* (brightness), a\* (green/red) and b\* (blue/yellow) were recorded. CIE values were converted into RGB values using a program (<<https://www.easyrgb.com/en/convert.php>>) to visualize the final colour of the films.

### 3.7. STATISTICAL ANALYSIS

The samples underwent triplicate analysis, and the results were presented as the mean  $\pm$  standard deviation. In cases involving two data groups, a Student's t-test was employed for comparison, while one-way analysis of variance (ANOVA) was applied when dealing with three or more groups. Assessment of normal distribution and variance homogeneity was carried out through the Shapiro–Wilk and Levene tests, respectively. When data exhibited homoscedasticity with  $p > 0.05$ , a Tukey's honestly significant difference (HSD) test was used. All statistical analyses were performed at a significance level of 5% using IBM SPSS Statistics software (Version 22.0, IBM Corp, Armonk, NY, USA).

## 4. RESULTS AND DISCUSSION

### 4.1. EXTRACT CHARACTERIZATION

The hydroethanolic extract obtained from *Prunus spinosa* L. was added to the films with the main objective of conferring them the capacity of changing their colour depending on the surrounding pH. In fact, anthocyanins have this particularity of presenting different colours depending on the structure they possess in specific conditions. However, these molecules are also well-known for their bioactive properties, often acting as antioxidant and antimicrobial agents, which are important properties when it comes to food preservation. Thus, in the present study, the extract was characterized not only in terms of anthocyanin profile, but also in terms of the additional benefits it can confer to the smart films.

#### 4.1.1. ANTHOCIANIN PROFILE

The anthocyanin profile of the extract, obtained by HPLC-DAD at 540 nm, is presented in **Figure 3**.

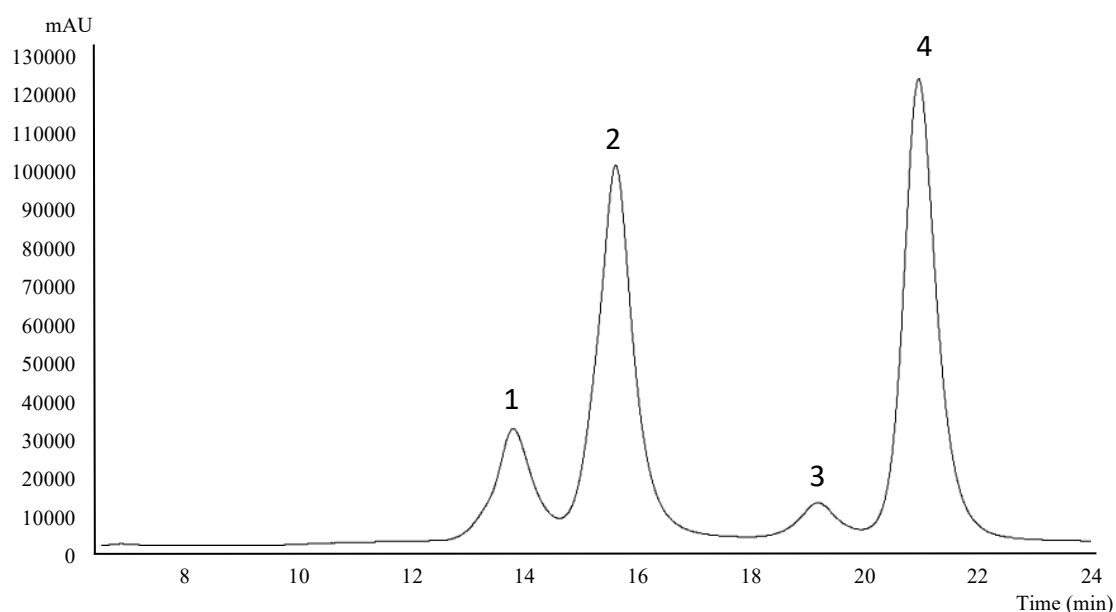


**Figure 3.** Anthocyanin chromatographic profile of the epicarp extract of *P. spinosa* fruits, obtained by HPLC-DAD at 520 nm.

The qualitative and quantitative characterization is detailed in **Table 5**.

**Table 5.** Anthocyanin tentative identification and quantification (in mg of compound per g of extract).

Peak	Rt (min)	$\lambda_{\text{m\acute{a}x}}$ (nm)	$[\text{H}]^+$ ( $m/z$ )	$\text{MS}^2$ ( $m/z$ )	Tentative identification	Quantification
1	13.68	517	449	287(100)	Cyanidin-3- <i>O</i> -glucoside	0.85±0.02 <sup>c</sup>
2	15.51	518	595	449(10),287(100)	Cyanidin-3- <i>O</i> -rutinoside	2.09±0.03 <sup>b</sup>
3	19.12	518	463	301(100)	Peonidin-3- <i>O</i> -glucoside	0.68±0.02 <sup>d</sup>
4	20.91	521	609	463(12),301(100)	Peonidin-3- <i>O</i> -rutinoside	4.43±0.07 <sup>a</sup>
<b>Total Anthocyanins</b>						<b>8.05±0.07</b>

ANOVA analysis—in the column, different letters indicate significant differences ( $p < 0.05$ ).

As shown in **Figure 3** and **Table 5**, cyanidin-3-*O*-rutinoside ( $[\text{M}+\text{H}]^+$  at  $m/z$  595) and peonidin-3-*O*-rutinoside ( $[\text{M}+\text{H}]^+$  at  $m/z$  609) were the major anthocyanins identified by HPLC-DAD-ESI/MS in extract obtained from the fruit epicarp of *P. spinosa*, followed by lower quantities of cyanidin-3-*O*-glucoside ( $[\text{M}+\text{H}]^+$  at  $m/z$  449) and peonidin-3-*O*-glucoside ( $[\text{M}+\text{H}]^+$  at  $m/z$  463).

The obtention of the extract was based on the optimization study previously carried out with the fruit in this research group. In this study (Leichtweis et al., 2019), optimization was performed in terms of the two majority compounds (Peaks 1 and 3), however the four compounds were also found in the chromatographic characterization of the fruit carried out by Guimarães et al. (2013).

These results (**Table 5**) corroborates to the valorisation of this wild fruit promoted by those studies (Guimarães et al., 2013; Leichtweis et al., 2019), with great potential for application of the extract in films.

#### 4.1.2. BIOACTIVITIES

To assess the antioxidant activity, the extract was tested through two *in vitro* assays, TBARS and DPPH, a cell-based and a chemical method, respectively (**Table 6**). In the TBARS method, the extract revealed a strong activity against lipid peroxidation, with an EC<sub>50</sub> value thirteen times lower than that presented by the positive control, Trolox (10.4 ± 0.5 and 139 ± 5 µg/mL, respectively). On the other hand, in terms of radical scavenging capacity, the extract and the positive control presented more approximate results, which is also a good result considering that this is a natural extract.

**Table 6.** Antioxidant activity of the *Prunus spinosa* extract (in µg/mL).

	DPPH	TBARS
Extract	40 ± 1 <sup>b</sup>	10.4 ± 0.5 <sup>b</sup>
Trolox	42 ± 1 <sup>a</sup>	139 ± 5 <sup>a</sup>

ANOVA analysis—in the column, different letters indicate significant differences (p < 0.05).

In terms of antimicrobial activity (**Table 7**), eight bacteria were used to assess the antimicrobial capacity of the extract and the best results were achieved against *Salmonella enterica*, which growth was inhibited by the *P. spinosa* extract at 2.5 mg/mL. *Escherichia coli* and *Staphylococcus aureus* were also sensitive to the extract at a concentration 5 mg/mL, and *Enterobacter cloacae* and *Listeria monocytogenes* were inhibited by a concentration of 10 mg/mL. The extract was not able to inhibit *Pseudomonas aeruginosa*, *Yersinia enterocolitica*, nor *Bacillus cereus*, at the maximum concentration tested (10 mg/mL).

**Table 7.** Antibacterial activity of the *Prunus spinosa* extract (in mg/mL).

	Extract		Streptomycin 1 mg/mL		Methicilin 1 mg/mL		Ampicillin 10 mg/mL	
	MIC	MBC	MIC	MBC	MIC	MBC	MIC	MBC
<i>Enterobacter cloacae</i>	10	>10	0.007	0.007	n.t.	n.t.	0.15	0.15
<i>Escherichia coli</i>	5	>10	0.01	0.01	n.t.	n.t.	0.15	0.15
<i>Pseudomonas aeruginosa</i>	>10	>10	0.06	0.06	n.t.	n.t.	0.63	0.63
<i>Salmonella enterica</i>	2.5	>10	0.007	0.007	n.t.	n.t.	0.15	0.15
<i>Yersinia enterocolitica</i>	>10	>10	0.007	0.007	n.t.	n.t.	0.15	0.15
<i>Bacillus cereus</i>	>10	>10	0.007	0.007	n.t.	n.t.	n.t.	n.t.
<i>Listeria monocytogenes</i>	10	>10	0.007	0.007	n.t.	n.t.	0.15	0.15
<i>Staphylococcus aureus</i>	5	>10	0.007	0.007	0.007	0.007	0.15	0.15

\*MIC- minimal inhibitory concentration; MBC – minimal bactericidal concentration.

Considering antifungal properties (**Table 8**), the extract was able to inhibit the growth of *Aspergillus fumigatus* and *Aspergillus brasiliensis* at a concentration of 5 and 10 mg/mL, respectively, and at 10 mg/mL it also presented fungicidal activity against *Aspergillus fumigatus*.

**Table 83.** Antifungal activity of the *Prunus spinosa* extract (in mg/mL).

	Extract		Ketoconazole	
	MIC	MFC	MIC	MFC
<i>Aspergillus brasiliensis</i>	10	>10	0.06	0.125
<i>Aspergillus fumigatus</i>	5	10	0.5	1

All the positive controls revealed stronger antimicrobial activity than the extract, which was expected for these antibiotics; nevertheless, comparing to other natural extracts, *P. spinosa* extract revealed an important activity, with no expected side effects often caused by synthetic molecules.

#### 4.2. FILM FORMULATIONS

Starch is made up of two glucose polymers: amylose, which is formed by glucose units linked by  $\alpha$ -1,4 glycosidic bonds, that is, a linear chain; and amylopectin, with a branched structure due to glucose units joined at  $\alpha$ -1,4 and  $\alpha$ -1,6. The utilization of starch in the fabrication of biofilms is based on the chemical, physical, and functional attributes of amylose to generate gels. This is because when amylose molecules are in solution, their linear structure promotes parallel alignment, allowing them to move closer together, thus facilitating the formation of hydrogen bonds between neighbouring polymeric hydroxyl

groups. Consequently, the polymer's affinity for water decreases, which promotes the creation of opaque pastes and robust films (Shimazu et al., 2007).

However, the use of starch to make flexible, malleable, and resistant films requires the addition of plasticizing agents that improve the mechanical properties of the film. Sorbitol and glycerol are among the most commonly studied and used, where the glycerol has already demonstrated better results (Lim et al., 2020).

In a brief literature search, it was possible to verify different ways of manufacturing the film based on cassava starch, where not only the quantities of the ingredients (starch, glycerol, and water) are important, but also the process parameters, more specifically the temperature and time in the gelation processes, and time, temperature and relative humidity in the film drying process. In the present study, five studies were selected to test these different parameters in order to reproduce the film with adequate characteristics, which are described in **Table 3**.

Initially, only control films were tested, that is, without the addition of anthocyanin extract, in order to verify the influence of manufacturing process parameters. For this, the different proportions of starch and glycerol diluted in 100 mL of water described in **Table 3** were used. The mixtures were then heated to the determined temperatures and for the times indicated by the authors, to obtain gelation of the starch in the mixture. The films were then placed in a Petri dish and taken to dry in an oven with relative humidity and controlled temperature, according to these conditions and drying times indicated. To expand the experiment, the individual protocols were not followed in the film thickness parameter, instead, quantities of 10, 20, and 30g of the mixture added to the Petri dish were tested, resulting in different film thicknesses in the different methodologies.

The differences between the films and the influence of the parameters were easily perceived by visual analysis of the films' characteristics. Basically, the appearance of the films was evaluated in terms of uniformity and mechanical resistance and flexibility during their handling. The main problem observed was the formation of bubbles in films whose protocols used high temperatures (Films 1, 2, 3, and 4). During the gelation process at temperatures equal to or higher than 90 °C, the films bubbled and the bubbles remained in the final (dry) film. To solve this problem, Yun et al. (2019) indicated the use of a degassing process, without further details, while Medina-Jaramillo et al. (2017) degassed the gel by applying vacuum for 7 min. However, bubbles were not observed in Film 5, in which low temperature and short time (1 min at 70 °C) were used, but with equal gel formation. Due to

the satisfactory visual homogeneity result, in addition to saving energy and an extra process step, these two conditions were chosen as optimal in this study.

Regarding the time, temperature, and relative humidity in the drying process, the effects were more dynamic. Films 2, 3, and 4, whose authors did not control relative humidity, were dried in a conventional oven with air circulation and renewal at 40 °C for 24 hours. Although these authors expressed good results, in the present study, an essential need to control humidity during drying process was verified, since the production of these films resulted in very brittle and not flexible films. Meanwhile, more promising results were achieved in Films 1 and 6, by controlling the relative humidity. However, the low temperature (30 °C) and high humidity ( $\geq 50$  °C) favour the appearance of mould in the films, in addition to requiring more drying time than reported by the authors. These problems required some adjustments, where by performing all the protocols with an increase in temperature to 40 °C and setting the relative humidity at 55% for 48h it was possible to obtain different films all with good drying aspects: films could be manipulated without breaking.

Once the influence of time, temperature, and relative humidity had been defined, all films were repeated under the established conditions to verify the influence of starch and glycerol contents, which until then were more subtle. Through this step it was possible to verify that the higher the addition of glycerol, the more flexible the film becomes, so that low amounts of glycerol resulted in rigid and less malleable films, while excess glycerol made them sticky and without structure. By varying the amount of glycerol between 7.95 and 22.05 g/100 g of cassava starch in their optimization study using a Rotational Composite Central Design, the authors of Film 4 (Queiroz et al., 2021) also found that high concentrations of glycerol gave greater manoeuvrability, lower force, and greater deformation when films break.

In sequence, the anthocyanin-rich extract obtained from *Prunus spinosa* epicarp was added to the film formulations. The addition of the extract was set in 1g of extract per film, which is the amount of extract verified to result in an intense and attractive purple colour on the films. The addition of the extract resulted in more malleable films, causing an effect similar to that of glycerol, which led to a decrease in the glycerol addition limit in relation to the control (without extract). Thus, for the final films, two formulations were defined, one with 25 and the other with 40 g/100g of starch, with 2 g of starch for 100 ml of water, as described in **Table 4**.

### 4.3. FILM CHARACTERIZATION

#### 4.3.1. THICKNESS

The films obtained as described in **Table 4** were measured by a digital micrometer, and the results are present in **Table 9**.

**Table 4.** Thickness of the film formulations.

Film	Thickness (mm)
0.5g-Control	0.090±0.008 <sup>a,A</sup>
0.8g-Control	0.08±0.05 <sup>a,B</sup>
0.5g-Anthoc	0.12±0.02 <sup>a,A</sup>
0.8g-Anthoc	0.12±0.01 <sup>a,A</sup>

ANOVA analysis—in each line, different small letters indicate significant differences ( $p < 0.05$ ) between film of the same type (control or extract-added), and different capital letters indicate significant differences ( $p < 0.05$ ) between the different types of film in terms of glycerol content.

It is possible to see that the little variation in the glycerol content did not change the film thickness for both types of control film and with added extract. However, it is notable that the addition of anthocyanins increased the film thickness, causing a difference, although small, significant ( $p < 0.05$ ) in “0.8g-Anthoc” in relation to the control (0.8g-Control). However, these differences were little or no noticeable during the manipulation of the films.

#### 4.3.2. FOURIER-TRANSFORM INFRARED SPECTROSCOPY (FTIR)

As presented in **Figure 4**, the spectra of the cassava starch film showed a band covering between 3700-3000  $\text{cm}^{-1}$ , namely at 3296  $\text{cm}^{-1}$ , due to the stretching vibration of the -OH group (Cheng et al., 2022; Lin et al., 2022). As starches are polymers formed by the condensation of glucose molecules, the specific peak of C-O-C bonds of glycosidic bonds was selected at 1145  $\text{cm}^{-1}$  (Cheng et al., 2022). The C-O-C bending of the  $\alpha$ -1,4 glycosidic bond was verified at wavelength 928  $\text{cm}^{-1}$ . Other characteristic peaks of cassava starch selected were: -CH stretching vibration of methyl group, C=O stretching vibration and stretching of the C-O band of aldehydes (Lin et al., 2022), at wavelengths 2890-2931, 1643 and 1077  $\text{cm}^{-1}$ , respectively.

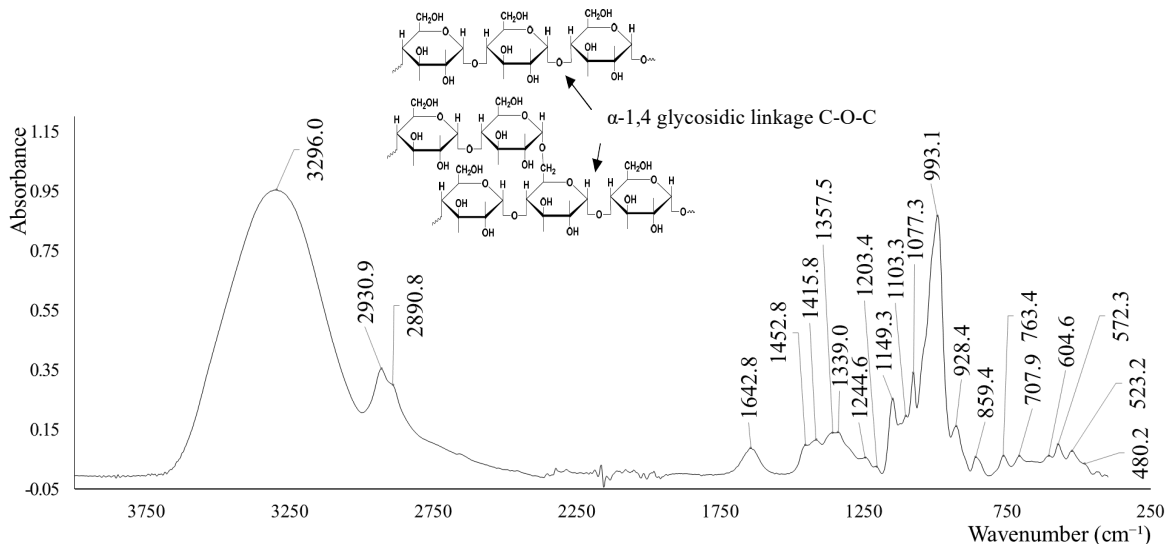


**Figure 4.** FTIR spectrum of cassava starch.

The FTIR spectrum of glycerol (**Figure 5**) showed a broad peak characteristic of -OH stretching from alcohol groups (Custódio et al., 2022), between 3100-3600 cm<sup>-1</sup>, namely at 3285.2 cm<sup>-1</sup>. The bands at 2932.4 and 2878.7 cm<sup>-1</sup> can be attributed, respectively, to the asymmetric and symmetric stretching of CH bonds; while the absorption bands at 1108.2 and 1029.6 cm<sup>-1</sup> correspond to the CO stretching of secondary and primary alcohol, respectively, as pointed out by Custódio et al. (2022).

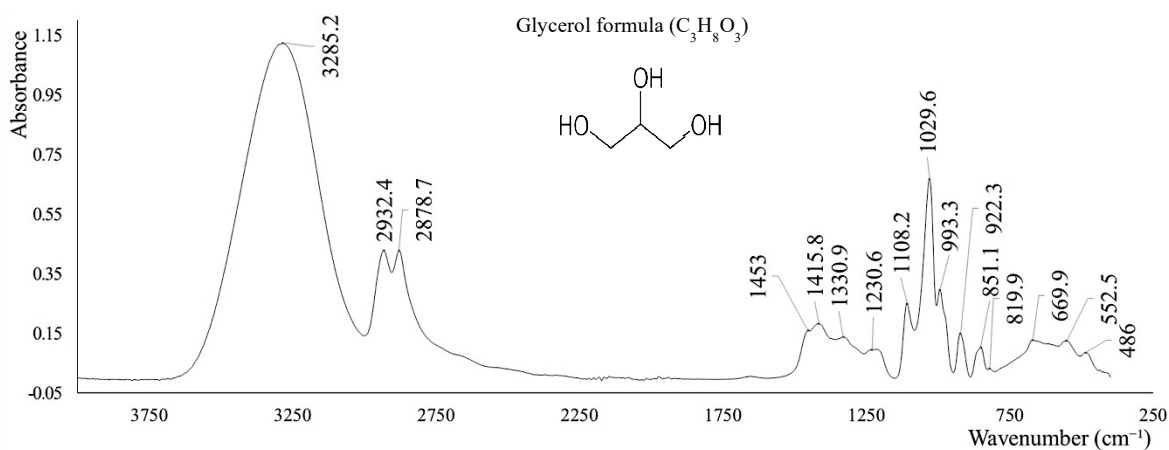


**Figure 5.** FTIR spectrum of glycerol.

Although the anthocyanin composition present in the extract used in the present study is mainly composed of peonidin-3-*O*-rutinoside and cyanidin-3-*O*-rutinoside, the FTIR spectrum was evaluated in terms of the basic chemical structure of anthocyanins, exemplified in **Figure 6**. This comparison is supported by a Bhushan et al. (2023) study, where the anthocyanins FTIR spectrum of purple or blue corn, which show strong bands at

certain wavelength, is not very different from the FTIR spectrum of red corn, with distinct absorbance bands (Bhushan et al., 2023).

The FTIR spectrum of the anthocyanin extract showed a broad band between 3100 - 3600  $\text{cm}^{-1}$ , namely at 3292.2  $\text{cm}^{-1}$ , associated with stretching vibrations of the -OH bonds. At 2931.7 and 2890.8  $\text{cm}^{-1}$ , two bands characteristic of the CH stretching vibration were observed and at 1717.7  $\text{cm}^{-1}$  the stretching vibration characteristic of the carbonyl ester group (C=O) was observed. The band at 1610.2  $\text{cm}^{-1}$  corresponded to the C=C bond of the central aromatic rings and represents the stretching vibration in the benzene rings; while the band observed at 1519.7  $\text{cm}^{-1}$  corresponds to the axial deformation of the C=C bond in aromatic rings. The bands between 1025.6-1153.2  $\text{cm}^{-1}$  were attributed to C–O bond tensions (Bhushan et al., 2023; Erna et al., 2022).

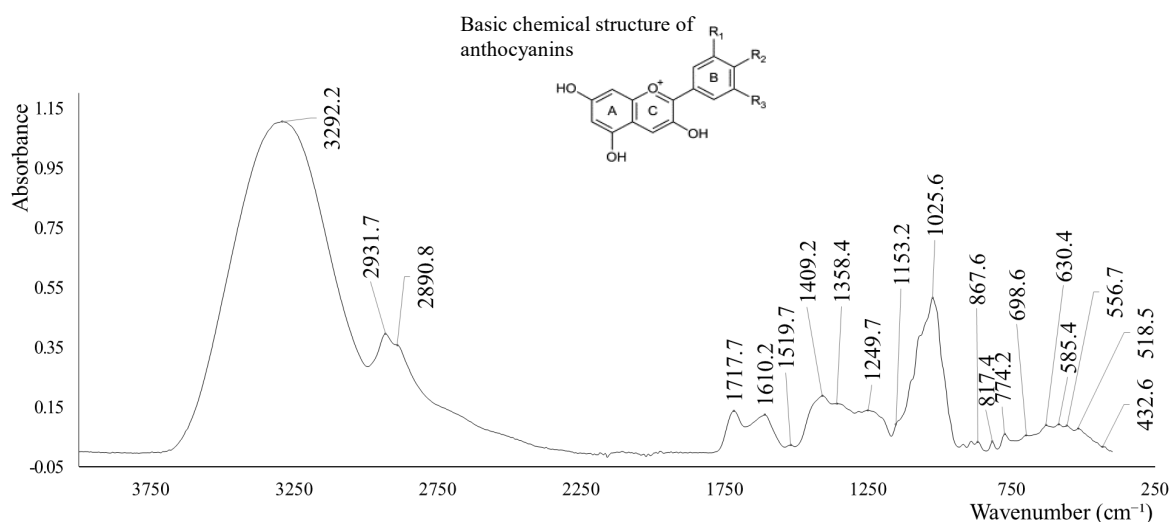


**Figure 6.** FTIR spectrum of the anthocyanin extract obtained from *P. spinosa* fruit epicarp.

In **Figure 7**, the FTIR spectrum of the “0.5g-Control” film formulation is compared with those of glycerol and cassava starch. Many of the glycerol bands overlapped with those of cassava starch, with the film showing characteristic bands of both compounds. The band at 2889.6  $\text{cm}^{-1}$ , referring to the -CH stretching vibration of the methyl group characteristic of cassava starch, had a slightly increased intensity, having been slightly shifted to 2880  $\text{cm}^{-1}$  in the biofilm. In the FTIR spectrum of the biofilm, the high intensity peak at 993.1  $\text{cm}^{-1}$  referring to the tension of the CO bond and bending of the C-O-H group of cassava starch had a reduced intensity, while the glycerol peak referring to the tension of the CO bond of C-OH groups, CC bond tension and C-OH bending at 1014.9  $\text{cm}^{-1}$ , was slightly shifted to 1012-1014  $\text{cm}^{-1}$ , with an increased intensity. The biofilm showed a broad band with two

high intensity peaks at 1014.4 and 997.7  $\text{cm}^{-1}$  referring to C-O bond tensions, C-C bond tensions and C-OH bond flexures. These peaks are characteristic of the biofilm and can be related to the interaction between its components, in which the FTIR spectra reflected: high intensity band at 1077.3  $\text{cm}^{-1}$  of cassava starch, high intensity band of glycerol at 1108.2  $\text{cm}^{-1}$  and band at 993.3  $\text{cm}^{-1}$ . Furthermore, the biofilm presented a broad band at 672  $\text{cm}^{-1}$ , evident only in the glycerol spectrum and referring to the bending of the C-C-O bonds of the pyranose ring. As pointed out by Erna et al. (2022), the increase in the intensity of the peaks is related to strong interactions, such as hydrogen bonds between the constituents of the biofilm, demonstrating the results obtained by scanning electron microscopy of the biofilm.

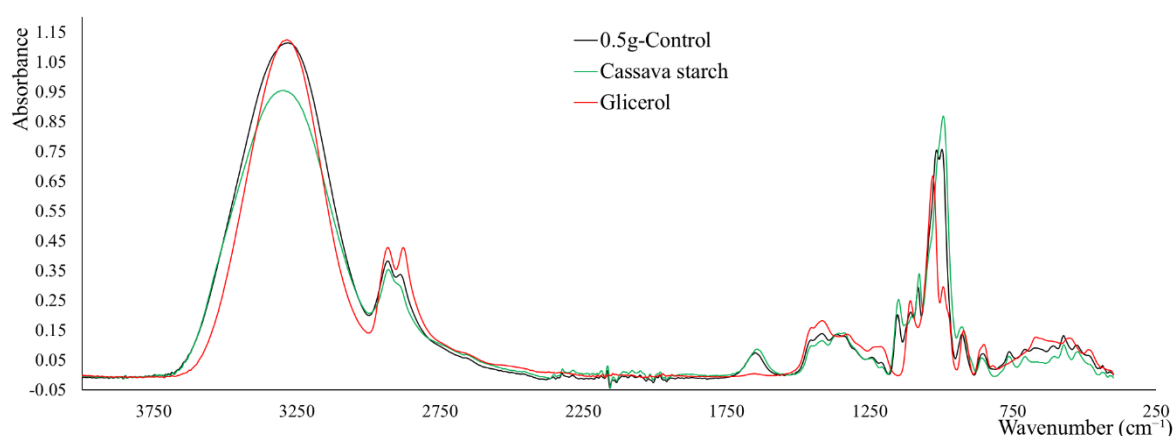


**Figure 7.** Comparison of FTIR spectra of the film “0.5g-Control”, the glycerol and the cassava starch.

The increase in the concentration of glycerol in the film (0.8g-Control) resulted in a slight reduction of the intensity of the bands at 2880 and 672  $\text{cm}^{-1}$ , while the band at 1015  $\text{cm}^{-1}$  overlapped with that of starch (**Figure 8**), showing that the film produced with a lower concentration of glycerol resulted in a greater interaction between starch and glycerol than in the present sample, which can be correlated to the micrograph of this biofilm (see 4.3.3).

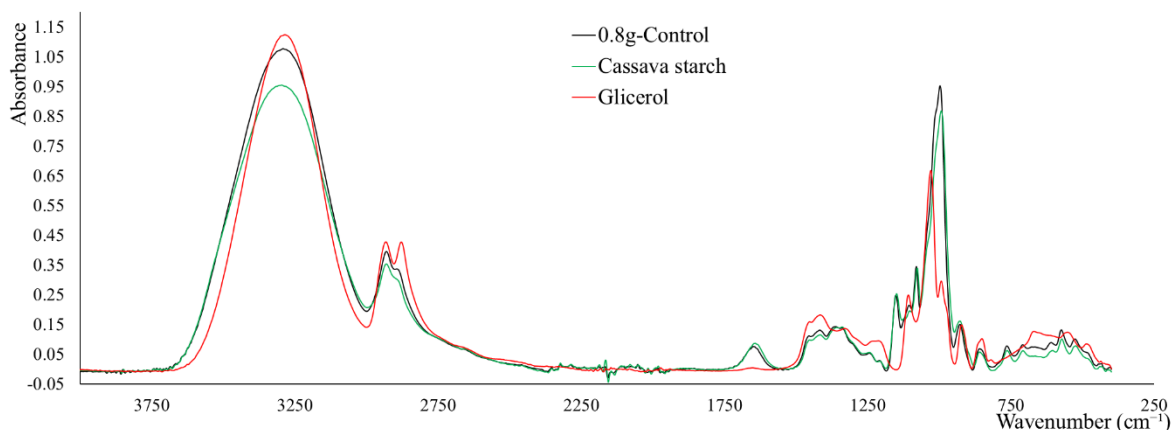


**Figure 8.** Comparison of FTIR spectra of the film “0.8g-Control”, the glycerol and the cassava starch.

The FTIR spectrum of the film produced with a lower concentration of glycerol and added with anthocyanin extract (0.5g-Anthoc) was compared with the spectra of the individual ingredients in **Figure 9**, and showed the characteristic bands of cassava starch, glycerol and anthocyanin extract. Typical bands were observed in the FTIR spectrum of cassava starch, with slightly lower intensity, such as those of the C-O-C bonds of glycosidic bonds at  $1149.3\text{ cm}^{-1}$  and the C-O-C bending of the  $\alpha$ -1.4 glycosidic bond at  $928.4\text{ cm}^{-1}$ . Typical and less intense bands of glycerol were also observed, such as the band at  $2878.7\text{ cm}^{-1}$  corresponding to the symmetric stretching of the CH bonds and the band at  $1029.6\text{ cm}^{-1}$  corresponding to the CO stretching of primary alcohol. Most of the typical bands of the anthocyanin extract overlapped with those of cassava starch and glycerol, making it possible to observe in the film a broad band of low intensity  $1717.7\text{ cm}^{-1}$ , characteristic of the extract, which was not observed in the film.

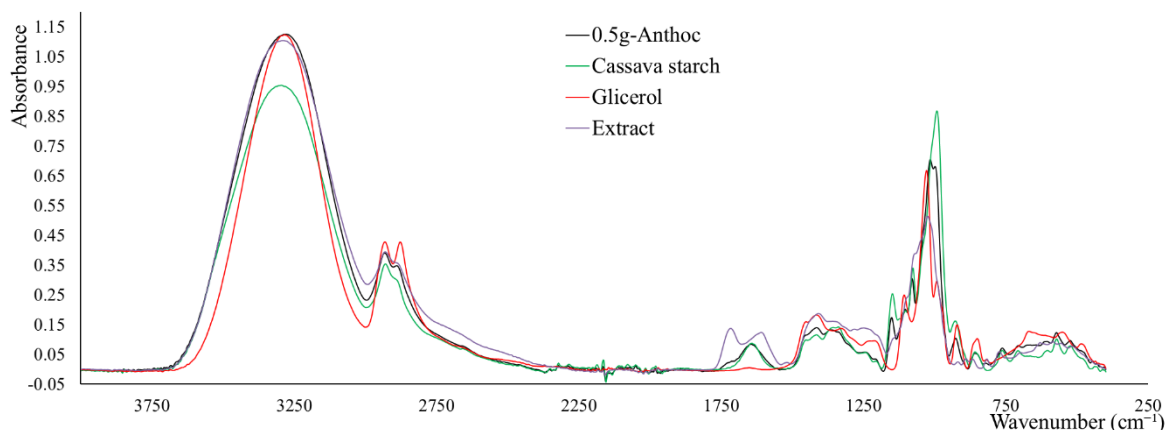


**Figure 9.** Comparison of FTIR spectra of the film “0.5g-Anthoc”, the glycerol, the cassava starch, and the anthocyanin extract obtained from *P. spinosa* epicarp.

Comparing films “0.5g-Anthoc” and “0.5g-Control” (with and without extract addition, respectively), in **Figure 10**, most bands overlapped. The bands at 1014.4 and 997.7  $\text{cm}^{-1}$ , characteristic of the film produced with cassava starch and 0.5g glycerol (0.5g-Control), are also verified in the FTIR spectrum of “0.5g-Anthoc” with slightly lower intensity, such as the bands at 925.5 and 857.6  $\text{cm}^{-1}$ , referring to the C-O-C bending of the  $\alpha$ -1,4 glycosidic bond and bending of the C-C-H and C-O-C bonds. On the other hand, the characteristic bands of glycerol, at 2931.4 and 2889.3  $\text{cm}^{-1}$ , showed slightly higher intensity in “0.5g-Anthoc”, as did the peak at 2659.8  $\text{cm}^{-1}$ , characteristic of the starch spectrum of cassava. The characteristic band of the extract at 1717.7  $\text{cm}^{-1}$  was also observed in the FTIR spectrum of “0.5g-Anthoc”. In general, the results suggest that it is possible to incorporate 33.3 g anthocyanin extract and 16.6g of glycerol per 100 g of starch into the cassava starch film.

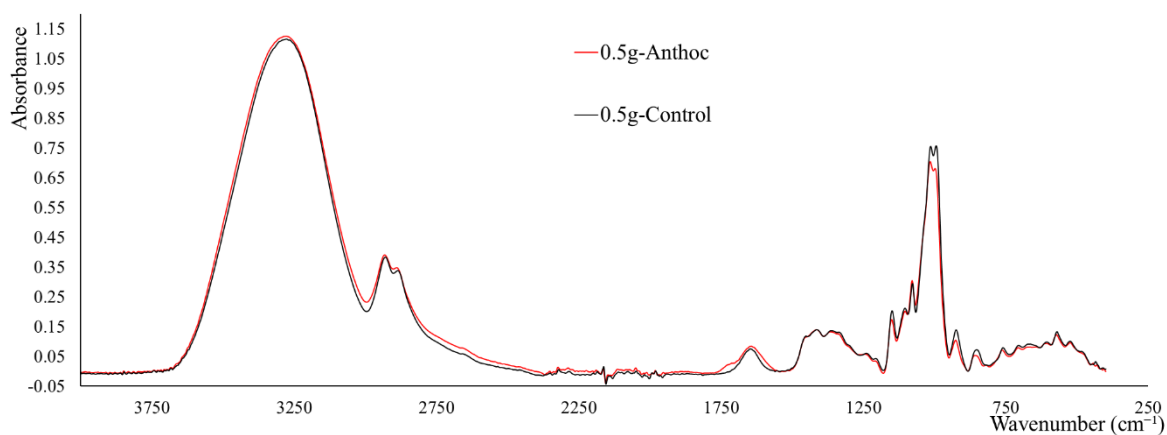


**Figure 10.** Comparison of FTIR spectra of the films “0.5g-Anthoc” and “0.5g-Control”.

The FTIR spectrum of the film produced with a higher concentration of glycerol and added with anthocyanin extract (0.8g-Anthoc) points to similarities to that observed for the “0.8g-Anthoc”: bands typical of starch cassava and glycerol and overlap of most bands in the anthocyanin extract spectrum, as seen in **Figure 11**. The typical band of the extract, stretching of the carbonyl ester group (C=O), was observed at wave number 1720.9  $\text{cm}^{-1}$ .

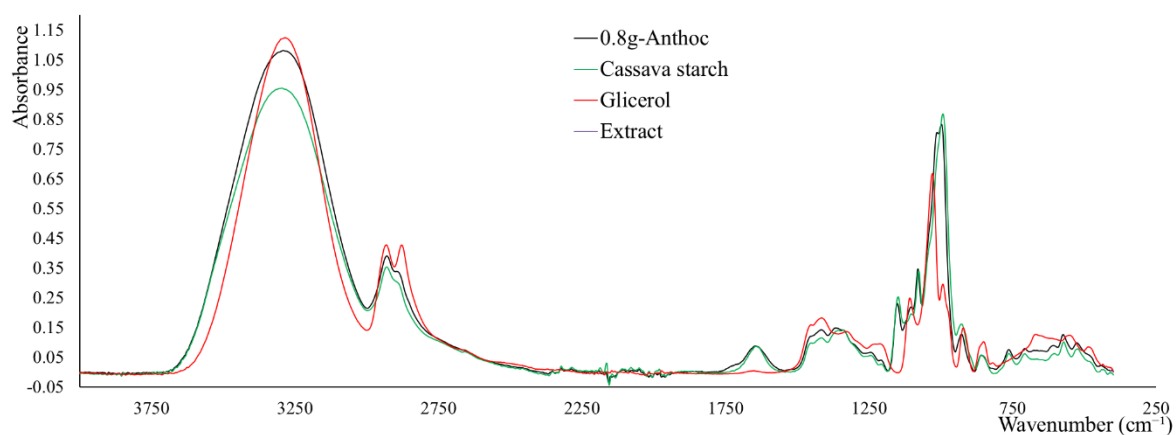


**Figure 11.** Comparison of FTIR spectra of the film “0.8g-Anthoc”, the glycerol, the cassava starch, and the anthocyanin extract obtained from *P. spinosa* epicarp.

Comparing films “0.8g-Anthoc” and “0.8g-Control”, in **Figure 12**, it is possible to notice that the bands at 1149.6  $\text{cm}^{-1}$  related to the asymmetric C-O-C tension of the glycosidic bond, 2928.3 and 2893.4  $\text{cm}^{-1}$ , characteristics of glycerol, showed a slight reduction in intensity; while the band related to the vibration of the bending of the C-OH bond and the tension of the C-O bond, characteristic of films, and observed at 1301.5  $\text{cm}^{-1}$ , had a slightly increased intensity. As in “0.5g-Anthoc”, the FTIR spectra of “0.8g-Anthoc” suggest the possibility of incorporating the extract into the film, at the studied concentrations.

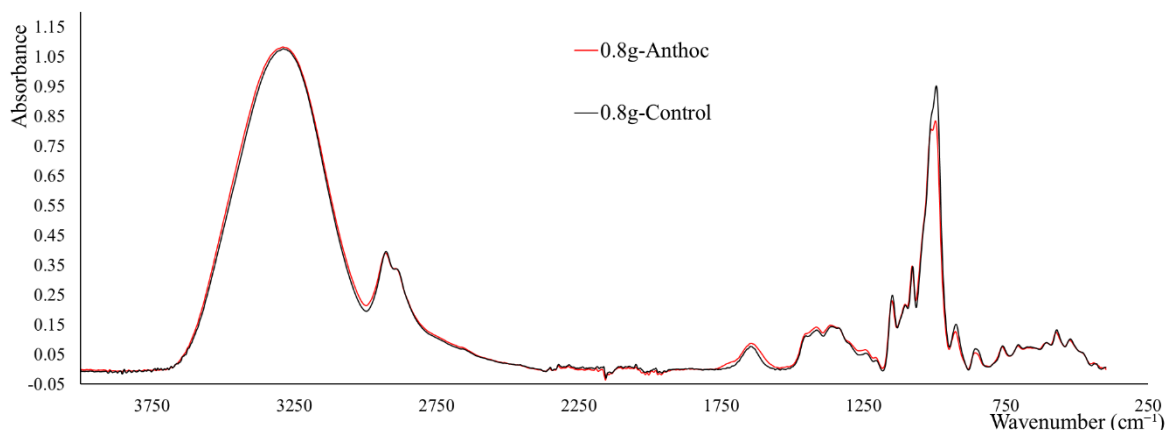


**Figure 12.** Comparison of FTIR spectra of the films “0.8g-Anthoc” and “0.8g-Control”.

#### 4.3.3. SCANNING ELECTRON MICROSCOPE (SEM)

**Figure 13** and **Figure 14** show the micrographs of the surface and the cross-section morphology, respectively, of starch-based films incorporated with anthocyanin extract. The micrographs from **Figure 13** revealed that all formulations showed roughness and ruptures in their structure. Also, it is possible to notice the presence of starch granules, especially in the control films, indicating that the addition of anthocyanin extract improves the gel solubility and the uniformity of the films. It is important to highlight that the samples were sensitive to the heat of the beam, which limited the ability to capture images at higher magnifications. In particular, areas more affected by beam heat compared to others within the same sample are observed. In general, films “0.5g-Anthoc” presented less rough and more homogeneous surface than “0.5g-Control”. While in film “0.8g-Control” it is possible to verify a higher sensibility through the presence of microcracks along the film in comparison to “0.8g-Anthoc”. The rougher structure of “0.8g-Control” than that of “0.5g-Control” corroborates the results verified by FTIR.

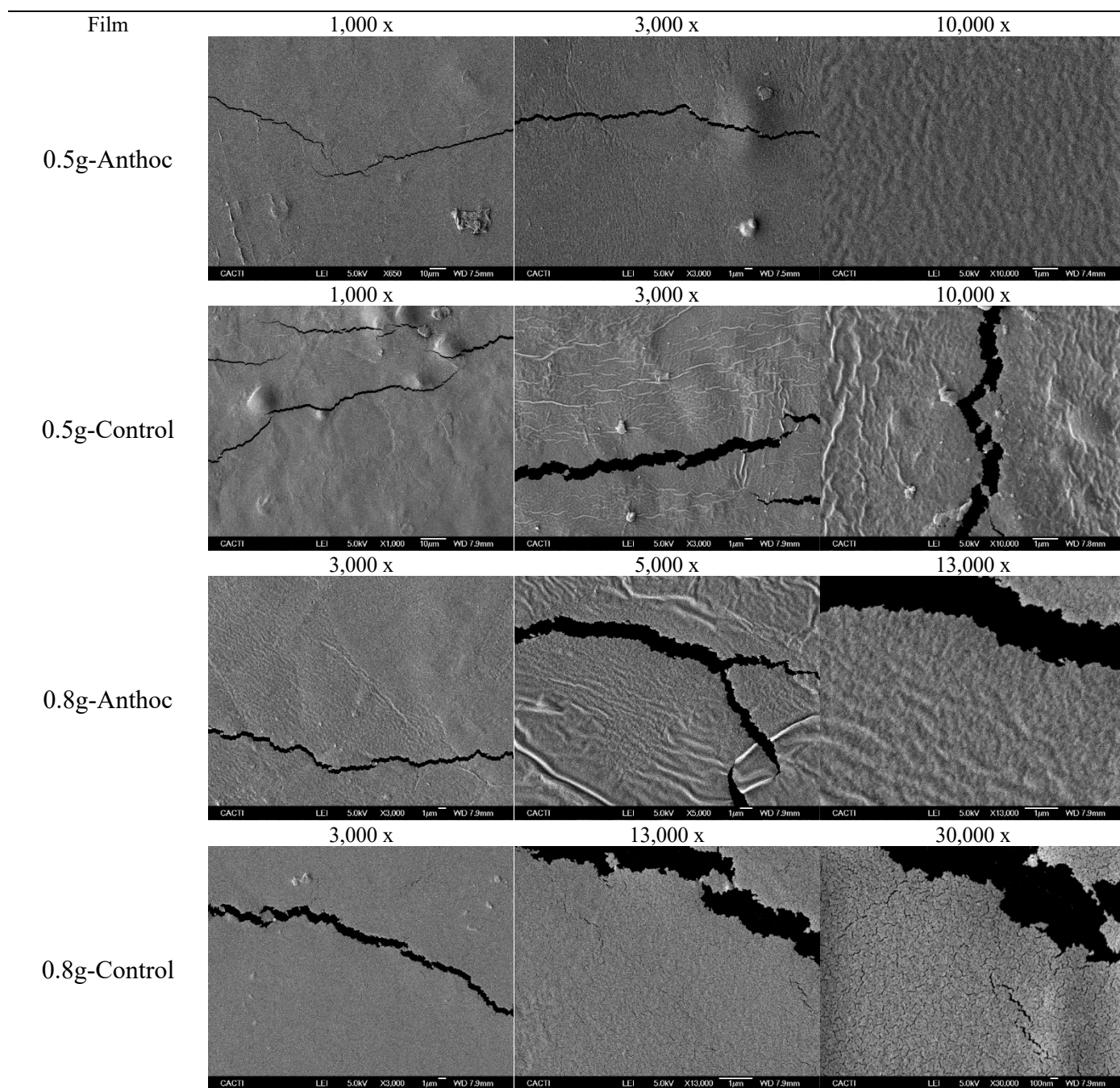


**Figure 13.** SEM of the surface of starch-based films incorporated with anthocyanin extract.

Despite the fractured structures, resulting from the overheating of the beam, through the cross-sectional images present in **Figure 5** it is possible to verify a denser, more compact, and more resistant structure in the “0.5g-Control” followed by “0.8g-Control”, as verified in the FTIR spectra (**Figures 10 and 12**). The addition of the anthocyanin-rich extract resulted in much rougher cross-sections as compared to the control films, also corroborating the FTIR spectra. In glycerol and starch films, Yun et al. (2019) found that the addition of low levels of anthocyanin-rich bayberry extract resulted in a flatter, denser cross-section in the film,

while the higher concentrations tested resulted in rougher cross-sections. In the present study, the extract concentration was the same in both films which varied in terms of glycerol concentration, pointing out its influence in cassava starch films.

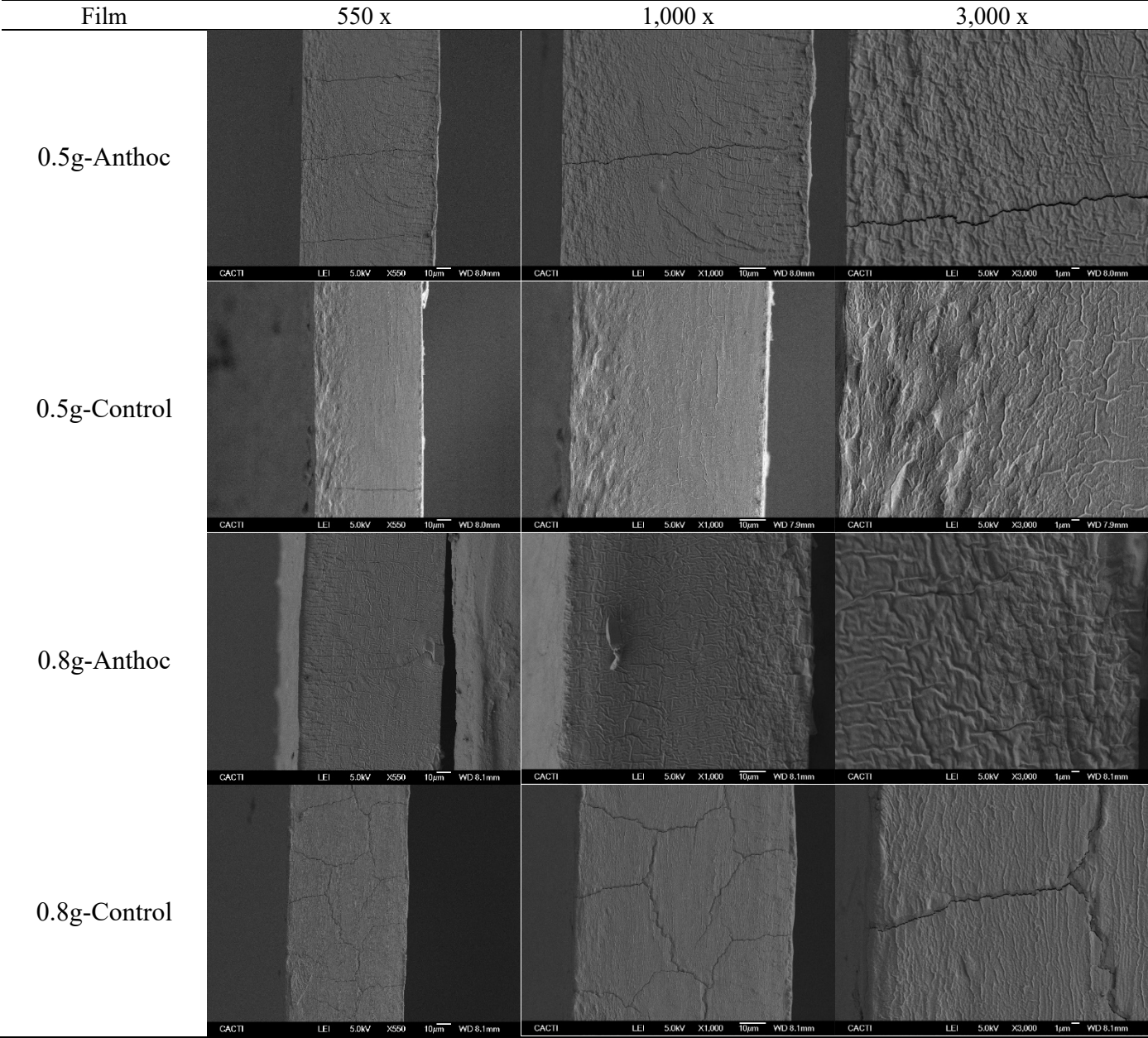


**Figure 14.** SEM of the cross-section morphology of starch-based films incorporated with anthocyanin extract.

4.3.4. pH SENSITIVITY

To verify the potential application of the film enriched with anthocyanin extract in monitoring pH variation, they were immersed in solutions with pH ranging from 1 to 12.

After the colour change occurred and stabilized, for approximately half an hour, the films were evaluated for their appearance and according to the CIE  $L^*$  (brightness),  $a^*$  (green/red) and  $b^*$  (blue/yellow) colour space values, also converted to RGB. As an example, **Figure 15** and **Table 10** present the results obtained for “0.5g-Anthoc”.

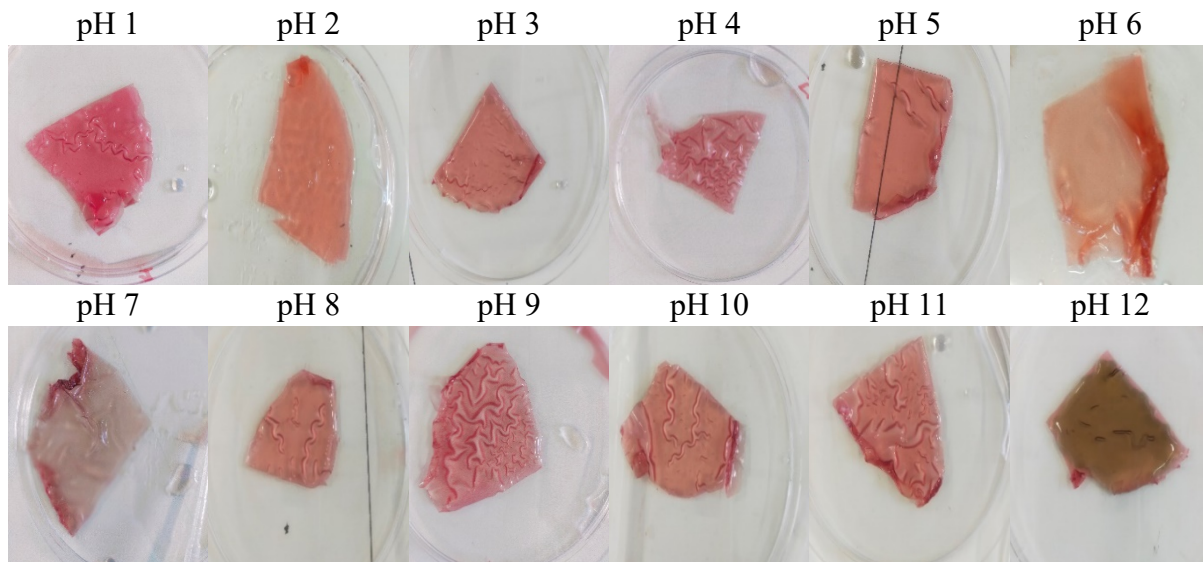


**Figure 15.** Effects in the colour of the film immersed in different buffer solutions.

**Table 5.** Effects in the colour of the film immersed in different buffer solutions.

	$L^*$	$a^*$	$b^*$	RGB
Initial film	36.1±0.2	11.0±0.2	6.9±0.2	
pH 1	66± 1	30± 2	21± 1	
pH 2	71.2± 0.5	23± 1	18.3± 0.9	
pH 3	68.5± 0.4	17.1± 0.8	21.2±0.8	
pH 4	71.3±0.7	18±1	17.4±0.5	
pH 5	72.0±0.5	20±1	19.3±0.5	
pH 6	75.6±0.6	14.1±0.9	18.0±0.7	
pH 7	74±1	7.6±0.6	15.2±0.5	
pH 8	75.3±0.3	13.6±0.2	17.4±0.2	
pH 9	75.5±0.3	7.5±0.7	16.2±0.6	
pH 10	76.6±0.2	13.7±0.9	18.1±0.9	
pH 11	75.2±0.4	12.6±0.2	17.2±0.1	
pH 12	60±2	9.8±0.8	17.4±0.8	

It is possible to notice that the colour of the film changes from red at pH 1 to 5 to more opaque colours at pH 6 to 10, and finally to yellow/green at pH 12. This change is attributed to alterations in the anthocyanin structure and the structural form of the anhydrous base (Zhang et al., 2019) . The initial red colour in acidic conditions is due to the predominant form of the original anthocyanin structure, known as the flavylium cation. A recent study

highlights pH as an essential determinant of anthocyanin coloration, given the ionic nature of the molecules that induce reversible or permanent structural changes depending on pH levels (Cavalcanti et al., 2011).

As reviewed by Erna et al. (2022), beyond a pH of 5, the red hue decreases to evolve into a greyish hue due to the emergence of a quinoidal base, while the flavylium cations dominate at pH 1-3, displaying a red colour. In contrast, deprotonation and hydration generate a pseudo-carbinol base at pH 4-5. A blue-violet hue characterizes the quinoid base, forming at pH 7-8. Beyond a pH of 12 to 14, the colour changes to yellowish-green, signalling the degradation of anthocyanins due to the high pH environment. This degradation causes the solution to adopt green or yellow hues. Anthocyanins are sensitive to pH, where the Pyridium cycle in their structure opens rapidly, producing a chalcone structure. This susceptibility is attributed to hydration and oxidation.

Cheng et al. (2022) also reported similar colour modifications in a similar study. In this study, the colour of all the films, based on cassava starch, glycerol, and red cabbage extracts, varied from pink to purple in buffer solutions with pH from 2 to 7, and further shifted from blue to yellow-green with pH from 8 to 12. By comparing the differences in the colour change of the films with the colour change observed in the crude extract immersed in the same buffer solutions, the author explained that it could be due to the hydrogen bonds formed between the compounds in the extract and the cassava starch which caused the changes in the anthocyanin structure.

## 5. CONCLUSIONS

This research has explored the promising trend of developing biodegradable smart films for packaging applications using cassava starch, glycerol, and an anthocyanin-rich extract obtained from *P. spinosa* epicarp. The anthocyanin extract, characterized by its predominant compounds cyanidin-3-*O*-rutinoside and peonidin-3-*O*-rutinoside, not only exhibited significant antimicrobial and antioxidant activities but also proved to be a suitable pH indicator for the smart films.

The formulation of films under advantageous conditions, considering factors such as gelation temperature, relative humidity during the drying process, and the proportion of ingredients, yielded homogeneous and cohesive films. The addition of glycerol influenced the FTIR spectra and surface morphology, while the incorporation of anthocyanins did not significantly alter the FTIR spectra, despite resulting in rougher surfaces observed by SEM.

Moreover, the films demonstrated a notable colour change in response to different pH solutions, reinforcing their potential for monitoring pH changes in products. This innovation revealed to be a promising way to address the environmental concerns associated with non-biodegradable packaging materials, offering a sustainable alternative that integrates the advantage of colour-based pH indication.

Overall, the successful development of these biodegradable smart films showcases a novel approach in food packaging technology, contributing to both environmental sustainability and enhanced food quality monitoring. Nevertheless, future studies are needed to assess the applicability of the developed films in different food matrices, as well as their intelligent properties, demonstrated by colour change caused by food degradation. Moreover, future research endeavours could further explore the scalability and commercial viability of this innovation in the food industry.

## 6. REFERENCES

- Ahmad, A., Dubey, P., Younis, K., & Yousuf, O. (2022). Mosambi (Citrus limetta) peel and Sago based biodegradable film: Development and characterization of physical, water barrier and biodegradation properties. *Bioresource Technology Reports*, 18, 101016. <https://doi.org/10.1016/J.BITEB.2022.101016>
- Andretta, R., Luchese, C. L., Tessaro, I. C., & Spada, J. C. (2019). Development and characterization of pH-indicator films based on cassava starch and blueberry residue by thermocompression. *Food Hydrocolloids*, 93, 317–324. <https://doi.org/10.1016/J.FOODHYD.2019.02.019>
- Arcos Coba, J. A., & Marín Cucalón, B. E. (2021). La actualidad de los tipos de envases plásticos para alimentos. *Journal of Engineering Science*, 3(6), 1–16. <https://doi.org/10.53734/esci.vol3.id176>
- Backes, E., Leichtweis, M. G., Pereira, C., Caroch, M., Barreira, J. C. M., Kamal Genena, A., José Baraldi, I., Filomena Barreiro, M., Barros, L., & C.F.R. Ferreira, I. (2020). Ficus carica L. and Prunus spinosa L. extracts as new anthocyanin-based food colorants: A thorough study in confectionery products. *Food Chemistry*, 333, 1274574. <https://doi.org/10.1016/j.foodchem.2020.127457>
- Bastos, C., Barros, L., Dueñas, M., Calhella, R. C., Queiroz, M. J. R. P., Santos-Buelga, C., & Ferreira, I. C. F. R. (2015). Chemical characterisation and bioactive properties of Prunus avium L.: The widely studied fruits and the unexplored stems. *Food Chemistry*, 173, 1045–1053. <https://doi.org/10.1016/j.foodchem.2014.10.145>
- Bhushan, B., Bibwe, B., Pal, A., Mahawar, M. K., Dagla, M. C., KR, Y., Jat, B. S., Kumar, P., Aggarwal, S. K., Singh, A., & Chaudhary, D. P. (2023). FTIR spectra, antioxidant capacity and degradation kinetics of maize anthocyanin extract under variable process conditions: Anthocyanin degradation under storage. *Applied Food Research*, 3(1), 100282. <https://doi.org/10.1016/j.afres.2023.100282>
- Bolumar, T., LaPeña, D., Skibsted, L. H., & Orlie, V. (2016). Rosemary and oxygen scavenger in active packaging for prevention of high-pressure induced lipid oxidation in pork patties. *Food Packaging and Shelf Life*, 7, 26–33. <https://doi.org/10.1016/J.FPSL.2016.01.002>
- Cardoso, G. P., Dutra, M. P., Fontes, P. R., Ramos, A. de L. S., Gomide, L. A. de M., & Ramos, E. M. (2016). Selection of a chitosan gelatin-based edible coating for color preservation of beef in retail display. *Meat Science*, 114, 85–94. <https://doi.org/10.1016/J.MEATSCI.2015.12.012>
- Cavalcanti, R. N., Santos, D. T., & Meireles, M. A. A. (2011). Non-thermal stabilization mechanisms of anthocyanins in model and food systems-An overview. *Food Research International*, 44(2), 499–509. <https://doi.org/10.1016/j.foodres.2010.12.007>
- Chen, H., Li, L., Ma, Y., McDonald, T. P., & Wang, Y. (2019). Development of active packaging film containing bioactive components encapsulated in  $\beta$ -cyclodextrin and its application. *Food Hydrocolloids*, 90, 360–366. <https://doi.org/10.1016/J.FOODHYD.2018.12.043>
- Cheng, M., Cui, Y., Yan, X., Zhang, R., Wang, J., & Wang, X. (2022). Effect of dual-modified cassava starches on intelligent packaging films containing red cabbage

- extracts. *Food Hydrocolloids*, 124(PA), 107225.  
<https://doi.org/10.1016/j.foodhyd.2021.107225>
- Custódio, A. C., Ribeiro, R. P. S., Lima, T. B. S. de, De, E. S., & Araújo, P. L. B. de A. (2022). Purificação Simplificada do Rejeito de Glicerina Bruta da Produção de Biodiesel da Biorrefinaria Berso-UFPE: Uma Prática Sustentável Simple Purification Process of Waste Glycerol from Berso-Ufpe Biorefinary Biodiesel Production: A Sustainable Practice Rev. *Revista Brasileira de Geografia Física V*, 15, 2226–2237.  
<https://periodicos.ufpe.br/revistas/rbgfe/article/viewFile/253719/41885>
- Deba, S., & Núñez, P. (2017). Efectos del bisfenol A en la reproducción femenina. *Medicina Reproductiva y Embriología Clínica*, 4(1), 52–58.  
<https://doi.org/10.1016/J.MEDRE.2017.02.001>
- Erna, K. H., Felicia, W. X. L., Vonnie, J. M., Rovina, K., Yin, K. W., & Nur'aqilah, M. N. (2022). Synthesis and Physicochemical Characterization of Polymer Film-Based Anthocyanin and Starch. *Biosensors*, 12(4). <https://doi.org/10.3390/bios12040211>
- Commission Regulation (EU) 2022/1616, Pub. L. No. Official Journal of the European Union 20.9.2022 L243 (2022). <https://www.efsa.europa.eu/en>
- Ezeoha, S. L., & Ezenwanne, J. N. (2013). Production of Biodegradable Plastic Packaging Film from Cassava Starch. *IOSR Journal of Engineering*, 3(10), 5–14. [www.iosrjen.org](http://www.iosrjen.org)
- Fang, Z., Zhao, Y., Warner, R. D., & Johnson, S. K. (2017). Active and intelligent packaging in meat industry. *Trends in Food Science & Technology*, 61, 60–71.  
<https://doi.org/10.1016/J.TIFS.2017.01.002>
- Geyer, R., Jambeck, J. R., & Law, K. L. (2017). Production, use, and fate of all plastics ever made. *Science Advances*, 3(7), e1700782.  
[https://doi.org/10.1126/SCIADV.1700782/SUPPL\\_FILE/1700782\\_SM.PDF](https://doi.org/10.1126/SCIADV.1700782/SUPPL_FILE/1700782_SM.PDF)
- Guimarães, R., Barros, L., Dueñas, M., Carvalho, A. M., Queiroz, M. J. R. P., Santos-Buelga, C., & Ferreira, I. C. F. R. (2013). Characterisation of phenolic compounds in wild fruits from Northeastern Portugal. *Food Chemistry*, 141(4), 3721–3730.
- Hahladakis, J. N., Velis, C. A., Weber, R., Iacovidou, E., & Purnell, P. (2018). An overview of chemical additives present in plastics: Migration, release, fate and environmental impact during their use, disposal and recycling. *Journal of Hazardous Materials*, 344, 179–199. <https://doi.org/10.1016/J.JHAZMAT.2017.10.014>
- Harrison, R. M., & Hester, R. E. (2018). *Plastics and the Environment* (R. M. Harrison & R. E. Hester (eds.); Vol. 47). Royal Society of Chemistry.
- Heising, J. K., Dekker, M., Bartels, P. V., & Van Boekel, M. A. J. S. (2012). A non-destructive ammonium detection method as indicator for freshness for packed fish: Application on cod. *Journal of Food Engineering*, 110(2), 254–261.  
<https://doi.org/10.1016/J.JFOODENG.2011.05.008>
- Heleno, S. A., Ferreira, I. C. F. R., Esteves, A. P., Ćirić, A., Glamočlija, J., Martins, A., Soković, M., & Queiroz, M. J. R. P. (2013). Antimicrobial and demelanizing activity of *Ganoderma lucidum* extract, p-hydroxybenzoic and cinnamic acids and their synthetic acetylated glucuronide methyl esters. *Food and Chemical Toxicology*, 58, 95–100. <https://doi.org/10.1016/j.fct.2013.04.025>
- Kim, H. S., Lee, K. Y., Jung, J. S., Sin, H. S., Lee, H. G., Jang, D. Y., Lee, S. H., Lim, K.

- M., & Choi, D. (2023). Comparison of migration and cumulative risk assessment of antioxidants, antioxidant degradation products, and other non-intentionally added substances from plastic food contact materials. *Food Packaging and Shelf Life*, 35, 101037. <https://doi.org/10.1016/J.FPSL.2023.101037>
- Konuk Takma, D., & Korel, F. (2019). Active packaging films as a carrier of black cumin essential oil: Development and effect on quality and shelf-life of chicken breast meat. *Food Packaging and Shelf Life*, 19, 210–217. <https://doi.org/10.1016/J.FPSL.2018.11.002>
- Krepker, M., Shemesh, R., Danin Poleg, Y., Kashi, Y., Vaxman, A., & Segal, E. (2017). Active food packaging films with synergistic antimicrobial activity. *Food Control*, 76, 117–126. <https://doi.org/10.1016/J.FOODCONT.2017.01.014>
- Lebreton, L., Slat, B., Ferrari, F., Sainte-Rose, B., Aitken, J., Marthouse, R., Hajbane, S., Cunsolo, S., Schwarz, A., Levivier, A., Noble, K., Debeljak, P., Maral, H., Schoeneich-Argent, R., Brambini, R., & Reisser, J. (2018). Evidence that the Great Pacific Garbage Patch is rapidly accumulating plastic. *Scientific Reports 2018 8:1*, 8(1), 1–15. <https://doi.org/10.1038/s41598-018-22939-w>
- Leichtweis, M. G., Pereira, C., Prieto, M. A., Barreiro, M. F., Baraldi, I. J., Barros, L., & Ferreira, I. C. F. R. (2019). Ultrasound as a rapid and low-cost extraction procedure to obtain anthocyanin-based colorants from *Prunus spinosa* L. fruit epicarp: comparative study with conventional heat-based extraction. *Molecules*, 24(3), 573. <https://doi.org/10.3390/molecules24030573>
- Li, C., Pei, J., Xiong, X., & Xue, F. (2020). Encapsulation of Grapefruit Essential Oil in Emulsion-Based Edible Film Prepared by Plum (*Pruni Domesticae* Semen) Seed Protein Isolate and Gum Acacia Conjugates. *Coatings 2020, Vol. 10, Page 784*, 10(8), 784. <https://doi.org/10.3390/COATINGS10080784>
- Lim, W. S., Ock, S. Y., Park, G. D., Lee, I. W., Lee, M. H., & Park, H. J. (2020). Heat-sealing property of cassava starch film plasticized with glycerol and sorbitol. *Food Packaging and Shelf Life*, 26, 100556. <https://doi.org/10.1016/J.FPSL.2020.100556>
- Lin, L., Peng, S., Shi, C., Li, C., Hua, Z., & Cui, H. (2022). Preparation and characterization of cassava starch/sodium carboxymethyl cellulose edible film incorporating apple polyphenols. *International Journal of Biological Macromolecules*, 212(March), 155–164. <https://doi.org/10.1016/j.ijbiomac.2022.05.121>
- Liu, K., Wang, X., & Young, M. (2014). Effect of bentonite/potassium sorbate coatings on the quality of mangos in storage at ambient temperature. *Journal of Food Engineering*, 137, 16–22. <https://doi.org/10.1016/J.JFOODENG.2014.03.024>
- Liu, X., Xu, Y., Liao, W., Guo, C., Gan, M., & Wang, Q. (2023). Preparation and characterization of chitosan/bacterial cellulose composite biodegradable films combined with curcumin and its application on preservation of strawberries. *Food Packaging and Shelf Life*, 35, 101006. <https://doi.org/10.1016/J.FPSL.2022.101006>
- Lora, A., Molina, A., Jos, A., Fernandez, R., Monterde, J., Blanco, A., & Moyano, R. (2010). Evaluation of the bisfenol-A gonadal toxic effect by histopathological study in zebrafish (*Danio rerio*). *Toxicology Letters*, 196, S333. <https://doi.org/10.1016/J.TOXLET.2010.03.1053>
- Luchese, C. L., Abdalla, V. F., Spada, J. C., & Tessaro, I. C. (2018). Evaluation of blueberry

- residue incorporated cassava starch film as pH indicator in different simulants and foodstuffs. *Food Hydrocolloids*, 82, 209–218. <https://doi.org/10.1016/J.FOODHYD.2018.04.010>
- Mamun, A. Al, Prasetya, T. A. E., Dewi, I. R., & Ahmad, M. (2023). Microplastics in human food chains: Food becoming a threat to health safety. *Science of The Total Environment*, 858, 159834. <https://doi.org/10.1016/J.SCITOTENV.2022.159834>
- Manalil, N. M., Dorado, M. A., & Otterdijk, R. van. (2011). Appropriated food packaging solutions for developing countries. *Food and Agriculture Organization of the United Nations (FAO)*. <http://dx.doi.org/10.1016/B978-0-12-088458-2.50010-2>
- Mangaraj, S., Yadav, A., Lalit, , Bal, M., Dash, · S K, & Mahanti, N. K. (2018). Application of Biodegradable Polymers in Food Packaging Industry: A Comprehensive Review. *Journal of Packaging Technology and Research* 2018 3:1, 3(1), 77–96. <https://doi.org/10.1007/S41783-018-0049-Y>
- Mas, S., Egido, J., & González-Parra, E. (2017). Importancia del bisfenol A, una toxina urémica de origen exógeno, en el paciente en hemodiálisis. *Nefrología*, 37(3), 229–234. <https://doi.org/10.1016/J.NEFRO.2017.01.011>
- Matheus, J. R. V., de Farias, P. M., Satoriva, J. M., de Andrade, C. J., & Fai, A. E. C. (2022). Cassava starch films for food packaging: Trends over the last decade and future research. *International Journal of Biological Macromolecules*, xxxx. <https://doi.org/10.1016/j.ijbiomac.2022.11.129>
- Matheus, J. R. V., de Farias, P. M., Satoriva, J. M., de Andrade, C. J., & Fai, A. E. C. (2023). Cassava starch films for food packaging: Trends over the last decade and future research. *International Journal of Biological Macromolecules*, 225, 658–672. <https://doi.org/10.1016/J.IJBIOMAC.2022.11.129>
- Medina-Jaramillo, C., Ochoa-Yepes, O., Bernal, C., & Famá, L. (2017). Active and smart biodegradable packaging based on starch and natural extracts. *Carbohydrate Polymers*, 176(August), 187–194. <https://doi.org/10.1016/j.carbpol.2017.08.079>
- NOAA. (2023). *What are microplastics?* National Ocean Service Website. <https://oceanservice.noaa.gov/facts/microplastics.html>
- Pack, E. C., Lee, K. Y., Jung, J. S., Jang, D. Y., Kim, H. S., Koo, Y. J., Lee, H. G., Kim, Y. S., Lim, K. M., Lee, S. H., & Choi, D. W. (2021). Determination of the migration of plastic additives and non-intentionally added substances into food simulants and the assessment of health risks from convenience food packaging. *Food Packaging and Shelf Life*, 30, 100736. <https://doi.org/10.1016/J.FPSL.2021.100736>
- Pires, T. C. S. P., Dias, M. I., Barros, L., Alves, M. J., Oliveira, M. B. P. P., Santos-Buelga, C., & Ferreira, I. C. F. R. (2018). Antioxidant and antimicrobial properties of dried Portuguese apple variety (Malus domestica Borkh. cv Bravo de Esmolfe). *Food Chemistry*, 240(August 2017), 701–706. <https://doi.org/10.1016/j.foodchem.2017.08.010>
- PlasticEurope. (2022). *Plastics – the Facts 2022*. Brussels. <https://plasticseurope.org/>
- Qin, Y., Liu, Y., Yong, H., Liu, J., Zhang, X., & Liu, J. (2019). Preparation and characterization of active and intelligent packaging films based on cassava starch and anthocyanins from Lycium ruthenicum Murr. *International Journal of Biological*

*Macromolecules*, 134, 80–90. <https://doi.org/10.1016/J.IJBIOMAC.2019.05.029>

- Queiroz, E. L., Araújo, G. S., Almeida, T. B., Martinez, E. A., & de Souza, S. M. A. (2021). Chemical and mechanical properties of cassava starch bioactive film with jambolan (*Syzygium cumini* L.) extract addition. *Brazilian Journal of Food Technology*, 24, 1–11. <https://doi.org/10.1590/1981-6723.21620>
- Risch, S. J. (2009). Food packaging history and innovations. *Journal of Agricultural and Food Chemistry*, 57(18), 8089–8092. <https://doi.org/10.1021/JF900040R>
- Rita, I., Pereira, C., Barros, L., Santos-Buelga, C., & Ferreira, I. C. F. R. (2016). *Mentha spicata* L. infusions as sources of antioxidant phenolic compounds: Emerging reserve lots with special harvest requirements. *Food and Function*, 7(10), 4188–4192. <https://doi.org/10.1039/c6fo00841k>
- Rossi, J., & Bianchini, A. (2022). “ Plastic waste free ” – A new circular model for the management of plastic packaging in food value chain. *Transportation Research Procedia*, 67, 153–162. <https://doi.org/10.1016/j.trpro.2022.12.046>
- Saha, N. C., Ghosh, A. K., Garg, M., & Sadhu, S. D. (2022). Food Packaging. In A. López-Paredes (Ed.), *Food packaging: materials, techniques and environmental issues*. Springer. <https://doi.org/10.1016/C2009-0-02704-4>
- Sarmiento, A., Barros, L., Fernandes, Â., Carvalho, A. M., & Ferreira, I. C. F. R. (2015). Valorization of traditional foods: Nutritional and bioactive properties of *Cicer arietinum* L. and *Lathyrus sativus* L. pulses. *Journal of the Science of Food and Agriculture*, 95(1), 179–185. <https://doi.org/10.1002/jsfa.6702>
- Sarra, H., & Ilham, H. (2022). *Élaboration et caractérisation d'un emballage comestible actif à base de mucilage d'Opuntia ficus indica et de la gomme de caroube*. Université de Tissemsilt.
- Sarria-Villa, R., & Gallo-Corredor, J. (2016). La gran problemática ambiental de los residuos plásticos: Microplásticos. *Journal de Ciencia e Ingeniería*, 8(1), 21–27. <https://jci.uniautonomia.edu.co/2016/2016-3.pdf>
- Shimazu, A. A., Mali, S., & Grossmann, M. V. E. (2007). Efeitos plastificante e antiplastificante do glicerol e do sorbitol em filmes biodegradáveis de amido de mandioca. *Semina: Ciências Agrárias*, 28(1), 79. <https://doi.org/10.5433/1679-0359.2007v28n1p79>
- Siracusa, V., Rocculi, P., Romani, S., & Rosa, M. D. (2008). Biodegradable polymers for food packaging: a review. *Trends in Food Science & Technology*, 19(12), 634–643. <https://doi.org/10.1016/J.TIFS.2008.07.003>
- Uwimbabazi, E., Mukasekuru, M. R., & Sun, X. (2017). Glucose Biosensor Based on a Glassy Carbon Electrode Modified with Multi-Walled Carbon Nanotubes-Chitosan for the Determination of Beef Freshness. *Food Analytical Methods*, 10(8), 2667–2676. <https://doi.org/10.1007/S12161-017-0793-6/TABLES/2>
- Vedove, T. M. A. R. D., Maniglia, B. C., & Tadini, C. C. (2021). Production of sustainable smart packaging based on cassava starch and anthocyanin by an extrusion process. *Journal of Food Engineering*, 289, 110274. <https://doi.org/10.1016/J.JFOODENG.2020.110274>
- Vicentini, N. M. [UNESP]. (2003). *Elaboração e caracterização de filmes comestíveis à base*

- de fécula de mandioca para uso em pós-colheita. *Aleph*, xvii, 198 f. : il., gráfs., tabs. <https://repositorio.unesp.br/handle/11449/103261>
- Vicentino, S. L., Floriano, P. A., Dragunski, D. C., & Caetano, J. (2011). Filmes de amidos de mandioca modificados para recobrimento e conservação de uvas. *Química Nova*, 34(8), 1309–1314. <https://doi.org/10.1590/s0100-40422011000800003>
- Wang, F., Xie, C., Tang, H., Hao, W., Wu, J., Sun, Y., Sun, J., Liu, Y., & Jiang, L. (2023). Development, characterization and application of intelligent/active packaging of chitosan/chitin nanofibers films containing eggplant anthocyanins. *Food Hydrocolloids*, 139, 108496. <https://doi.org/10.1016/J.FOODHYD.2023.108496>
- Waring, R. H., Harris, R. M., & Mitchell, S. C. (2018). Plastic contamination of the food chain: A threat to human health? *Maturitas*, 115, 64–68. <https://doi.org/10.1016/J.MATURITAS.2018.06.010>
- Weston, M., Kuchel, R. P., Ciftci, M., Boyer, C., & Chandrawati, R. (2020). A polydiacetylene-based colorimetric sensor as an active use-by date indicator for milk. *Journal of Colloid and Interface Science*, 572, 31–38. <https://doi.org/10.1016/J.JCIS.2020.03.040>
- Yadav, V., Sherly, M. A., Ranjan, P., Tinoco, R. O., Boldrin, A., Damgaard, A., & Laurent, A. (2020). Framework for quantifying environmental losses of plastics from landfills. *Resources, Conservation and Recycling*, 161, 104914. <https://doi.org/10.1016/J.RESCONREC.2020.104914>
- Yun, D., Cai, H., Liu, Y., Xiao, L., Song, J., & Liu, J. (2019). Development of active and intelligent films based on cassava starch and Chinese bayberry (: *Myrica rubra* Sieb. et Zucc.) anthocyanins. *RSC Advances*, 9(53), 30905–30916. <https://doi.org/10.1039/c9ra06628d>
- Zhang, J., Zou, X., Zhai, X., Huang, X. W., Jiang, C., & Holmes, M. (2019). Preparation of an intelligent pH film based on biodegradable polymers and roselle anthocyanins for monitoring pork freshness. *Food Chemistry*, 272(April 2018), 306–312. <https://doi.org/10.1016/j.foodchem.2018.08.041>
- Zhao, L., Liu, Y., Zhao, L., & Wang, Y. (2022). Anthocyanin-based pH-sensitive smart packaging films for monitoring food freshness. *Journal of Agriculture and Food Research*, 9, 100340. <https://doi.org/10.1016/J.JAFR.2022.100340>